CHAPTER 5

Reclamation of Copper from Spent Ammoniacal Printed Circuit Board Etch Solutions

Almost one billion cubic meter of waste etchant is being generated annually from the PCB industry with an increase in 15–18% (Yu et al., 2016). Therefore, it is imperative to reclaim copper to the fullest extent from such wastes and discards. This Chapter focuses on the recovery of copper from spent etching solutions using the solvent extraction technique. Solvent regeneration by the precipitation–stripping technique eventually reclaims the copper as copper oxide that has considerable commercial potential. Use of copper oxide as catalyst for reduction reactions is also explored.

5.1 Introduction

Electronic devices encompass every aspect of human life and are built on the foundation of Printed Circuit Boards (PCBs) which carries the electronic architecture of the device with copper as the main conducting material. The copper concentration in PCB varies depending on the number of layers and the capacity of conductor current (Hadi *et al.*, 2015) and it is usually about 15-35% by weight (Isildar *et al*., 2017) of PCB. This copper content is far greater in comparison to the 3% copper in most of the newly mined ores (Shokri *et al*., 2017). According to Institute of Printed Circuits (IPC) the world PCB market reached an estimated $58.2 billion in 2016. The worldwide output of PCBs has increased by an average of 8.7% each year and will continue to increase (Wang *et al.*, 2017) resulting in an increased use of copper. International Copper Study Group (ICSG) projections indicate a copper deficit of 150,000T for 2017 and 105,000T in 2018.

The Indian electronics market is one of the fastest growing in the world and is anticipated to reach US$ 400 billion in 2022, with domestic manufacturing climbing to over US$ 100 billion. According to an Electronics Industries Association of India (ELCINA) study, domestic market demand for PCBs will grow at a CAGR of 20.56 % over the period 2015-2020, and will reach over US$ 6 billion by 2020 from the current level of US$ 2.38 billion.

PCBs are essential component of all electrical and electronic equipment and are present in TVs, computers, smartphones, mobile phones, washing machines, refrigerators etc. Figure 5.1 shows the weight percent PCB in electronic items. PCBs consist of approximately 40 wt% of metals, 30 wt% of plastics, and 30wt% ceramics (He *et al.*, 2006). They are made up of glass fibre-enhanced epoxy and metals which include precious metals (Choubey *et al.*, 2015; Gu *et al.*, 2016). They support and connect the electronic components via conductive tracks, on etched copper sheets laminated onto a non-conductive glass-fibre reinforced epoxy resin substrate (Hall and Williams, 2007).

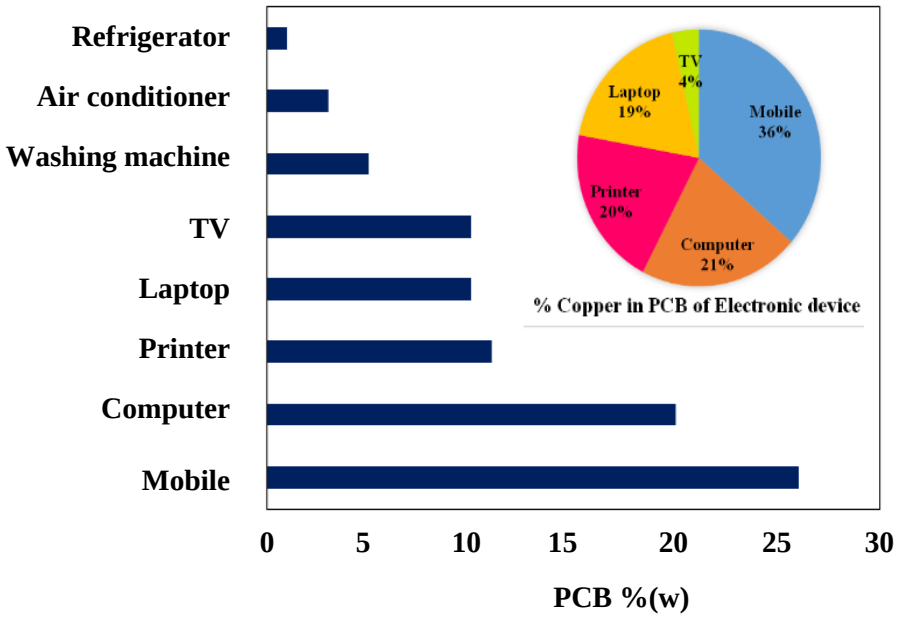

Fig.5.1: PCB (%w) in consumer products and copper content in PCB

Bare PCB substrates represent an average 23% of the total board weight (Duan *et al.*, 2011). Metal concentrations in PCBs depend on their source, type of the board, manufacturer, and period of production (Isildar, 2018). Modern electronic equipments are found to contain 60 different elements of which Cu, Ni, Fe, Pb, Ag, Au, Zn, etc. are most frequently used as indispensable parts in various electronic industries (Chobey, 2015). Copper content in PCB is around 10-20%.

Figure 5.1 (inset) shows the copper share in PCBs of various electronic items. Lead/Tin solders used for joining different components account for 4-6% of the total weight. Nickel is used in contacts as an additive. Beryllium as its oxide and aluminium are used for their heat conductivity (Isaldar *et al.*, 2016). Tin is also located on the surface of PCB (Marques,

2013). The most common metal components present in PCB and their functions are shown in Figure 5.2.

Precious metals Au and Pd are used as contact materials in joints (Ghosh *et al.*, 2015). Concentration of precious metals in waste PCBs is higher than the concentration of precious metals in their ores (Chancerel *et al.*, 2009). PCBs also contain different metallic values such as Ga, In, Ti, Si, Ge, As, Se and Te. A detailed overview of the metals presents in PCBs compiled from different literature sources is reported by Stuhlpfarrer *et al.*, 2015. Isildar *et al.* (2018) have presented an overview of the metals present in electronic items along with their concentrations.

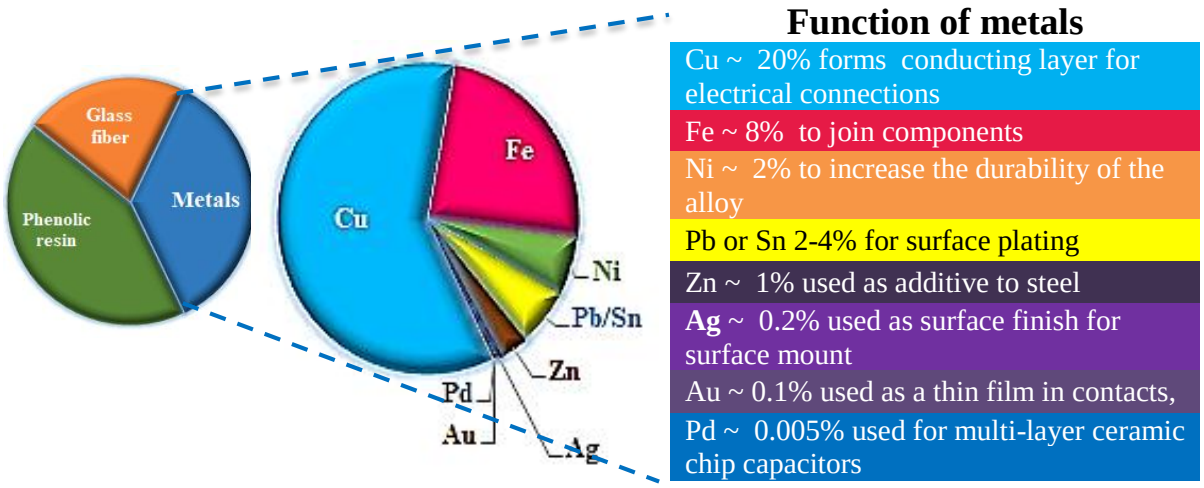

Fig. 5.2: Metal components in PCB and their functions

5.2 PCB classification and manufacturing process

PCBs are classified depending on the number of layers as single layer board, double layer board wherein circuits with two layers of copper are linked by metallized holes, and multi layered boards in which the circuits are placed in multiple layers on a single board (Nakahara, 2007). Some boards have even as many as 50 layers each with its own circuit patterns (Khandpur, 2006). Layer count is the most common way of categorizing PCBs; higher layer counts require more sophisticated fabrication technology. In India PCB manufacturers mostly produce single-sided, double-sided and multi-layered PCBs that could go up to a layer count of four to six.

PCBs are also classified on the basis of type of substrates as rigid and flexible. In recent times flexible boards are popular due to the advantage of being shaped into different configurations. Though the manufacturing processes are the same (La Dou, 2006), rigid boards are costlier than the flexible ones. Indian manufacturers mostly adopt the high-mix, medium-volume strategy where different types of PCBs are manufactured in low to medium volumes. There are around 200 PCB manufacturers in India of which more than 60 per cent are very small and in the unorganized sector. (The Indian PCB industry Challenges and Opportunities, 21 March 2017)

PCB manufacturing is a complex process and requires more than fifty steps (La Dou, 2006) depending on the application and complexity therein from cleaning to quality control (Schuerink *et al.*, 2013). In general, the main steps involved are drilling, scrubbing, chemical cleaning, electroless deposition, photo imaging, pattern plating, resist stripping, and etching (Stone, 1990). PCB Manufacturing processes are classified as additive or subtractive. Subtractive process involves plating a substrate with conductive copper and then exposing it to electrolytic plating. The substrate circuit pattern can be created by masking and etching. In the additive process, copper is deposited selectively on the base laminate, depending on the design of the circuit. The additive process metalizes the substrates through holes and the circuitry pattern at the same time, thereby eliminating the need for electroplating. This process can produce finer lines in comparison to the boards produced by the standard etching process. It has the ability to metallize high aspect ratio holes uniformly (Khandpur, 2006). The use of additive plating will increase, with the demand for high-density PCBs.

5.3 PCB etching process

Etching is one of the major steps in the chemical processing of subtractive PCB process. Etching process is used to develop the circuit pattern in PCBs by removing the excess portion of copper from the copper clad laminate (Panias *et al.,* 2002). Chemical, electrochemical and mechanical are the major etching methods used.

Etching process is carried out by immersion, bubble, splash or spray method (Khandpur, 2006). Immersion etching is the simplest method wherein the boards are suspended vertically from a rack in a tank and a long process time is required. A modified immersion etching process is bubble etching, here the boards are held vertically by a rack. During

etching process air is bubbled through the etch solution which provides oxygen and increases the etch rate. In splash etching the etch solution is splashed using centrifugal force which results in even etching and less undercut however, the process is slow and is now obsolete. Due to its high productivity, fast rate and fine line etching, spray method is widely used. In this process the etchant is pumped under pressure through nozzles. The boards can be placed horizontally or vertically and etching time required is less (Khandpur, 2006).

The copper dissolved away by etching process depends on the design and the type of board and is about 50–70% of that originally present on the board (Giannopoulou *et al*., 2003). This indicates large amount of copper containing etchant being generated during manufacturing. In etching copper, the most important parameter is etch rate. The choice of the etchant depends on its availability as well as the structure of PCB (Keskitalo *et al*., 2007). The properties of an ideal etchant include high etch rate, minimum undercut, high dissolved copper capacity, easy control, economic regeneration of waste etch and copper recovery (Cakir, 2003). Yu *et al*. (2016) have categorised the etchants chronologically in three classes as (1) previously used (ferric chloride, ammonium persulfate, hydrogen peroxide- sulfuric acid, chromic disulfuric acid, sodium chlorite), (2) currently used (cupric chloride and alkaline ammonical ammonium chloride) and (3) emerging etchants (chlorine /hydrochloric acid). Alkaline ammonia based etchant and cupric chloride acid based etchant are currently the most extensively used copper etchants (LaDou, 2006).

Cupric chloride etchant is used for large scale operations. It is compatible with photopolymer resists and is used for fine-line multilayer inner etching, print-and-etch boards, and panel-plate/tent-and-etch boards. Due to buildup of cuprous ions, etching becomes slow, hence, this etchant is always used in a regenerative system with continuous oxidizer management and control. However, increasing the etching temperatures increases the etch rate. (Cakir, 2003).

In cupric chloride etching copper is etched by using a solution of copper itself, due to the fact that copper can transform from one oxidation state to other. Elemental copper reacts with cupric copper to form cuprous copper and copper accumulates in the solution whereas copper ions responsible for etching are reduced. To maintain the required, etch rate cuprous copper is converted to cupric state by regeneration so that it can etch more metal (Keskitalo *et al*., 2007). The overall etching reaction wherein cupric chloride ($CuCl_2$) dissolves copper (Cu) is given by Equation 5.1

$$Cu + CuCl_2 \rightarrow 2CuCl \quad (5.1)$$

Alkaline ammonium chloride etching solutions were commercialized after 1977. Alkaline ammonical etching is compatible with metallic and organic resist. Due to high copper dissolving capacity the system is increasingly used in the PCB industry. Alkaline etching solution dissolve exposed copper by a chemical process involving oxidation, solubilizing and complexation to form cupric ammonium complex which hold the etched and dissolved copper in the solution (Equation 5.2, Equation 5.3). Post etching rinsing is critical leading to waste treatment problems due to the presence of ammonium ion.

$$Cu + (CuNH_3)_4^{2+} \rightarrow 2Cu(NH_3)_4^{+} \quad (5.2)$$

$$4(CuNH_3)_2^{+} + 8NH_3 + O_2 + 2H_2O \rightarrow 4(CuNH_3)_4^{+2} + 4OH^{-} \quad (5.3)$$

Table 5.1 lists the components, advantages and disadvantages of different etchants used in the PCB industry (Cakir, 2003; Khandpur 2005; Coombs, 2007; Keskitalo *et al.*, 2007, Clark 2012; Yu *et al.*, 2016).

5.4 Regeneration strategies and copper recovery from spent etch solutions

Alkaline ammonia based and cupric chloride acid based etchants are currently the most widely used copper etchants in the PCB manufacturing processes. During cupric chloride etching the build-up of cuprous ion slows down the etching process. In order to maintain a constant rate a regenerative system must be used. Regeneration in this case is somewhat complex.

The regeneration of the etchant is achieved by reoxidizing the cuprous chloride to cupric chloride by air oxidation (Equation 5.4), direct chlorination (Equation 5.5), using sodium chlorate (Equation 5.6), hydrogen peroxide (Equation 5.7) and electrolytic regeneration. In the process, a small amount of solution is continuously drained off to keep the concentration of copper constant.

$$2CuCl_2 + 4HCl + O_2 \rightarrow 4CuCl_2 + 2H_2O \quad (5.4)$$

$$Cl_2 + Cl_2 \rightarrow 2CuCl_2 \quad (5.5)$$

$$3Cu_2Cl_2 + NaClO_3 + 6HCl \rightarrow 6CuCl_2 + NaCl + 3H_2O \quad (5.6)$$

$$Cu_2Cl_2 + 2H_2O_2 + 2HCl \rightarrow 2CuCl_2 + 2H_2O \quad (5.7)$$

Table 5.1: Advantages and disadvantages of etchants used during PCB etching process

Etchant	Components	Advantages	Disadvantages
Ferric chloride	ρ-1.35 to1.4 Cu-120g/l HCl-10ml/l, T 20-45^{0}C Anti-foaming agent-3ml/l	• High metal holding capacity. • High etching rate.	• Attacks tin so not suitable for Sn/Pb plated boards. • Corrosive. • Difficult to regenerate. • Disposal is expensive.
Ammonium persulfate	$(NH_4)_2 S_2O_8$-200 g/l H_2SO_4-10 ml/L H_2Cl_2-0.5 ml/L T-30 to 40 ^{0}C	• Overcomes the disadvantages of ferric chloride as etchant.	• Unstable at high temperature and high copper concentration. • High cost.
Hydrogen peroxide-sulfuric acid	H_2SO_4-100ml/L H_2O_2-70ml/l CuSO4-60g/l, T-30 to 40 ^{0}C	• Compatible with organic and metallic resist. • Steady etch rate. • Optimum undercut.	• Difficult etchant composition balance • Handling of concentrated peroxide solution • Not used for Pb-Sn alloys
Chromic-sulfuric acid	Chromic acid-200 to 240g/l H_2SO_4-60 to 65 ml/l Na_2SO_4-40 to 45 g/l T-20 to 30 ^{0}C	• Little undercutting. • Used for all metal resists.	• Inconsistent etching rate. • Difficult to regenerate. • Highly toxic and hazardous. • Serious disposal problem.
Cupric chloride	$CuCl_2$-200 g/ L HCl-200 ml/L Water-770 m/L Cu -40 g/L H_2O_2-30ml/L (optional) T-30 to 40 ^{0}C	• For board having close traces, over etching or undercutting of traces is not there. • Fine line etching is achieved. • Longer solution service life. • Can retain more copper before it becomes spent. • Easy regeneration.	• Not used for outer layer processing as it strips Pb/Sn solders that protects the copper surface.
Ammonium chloride	NH_4HCO_3-75g/L NH_4NO_3- 80g/L Cupric chloride-200g/L NH_4Cl-100-110g/L T-45to55℃ pH- 7.8-8.2 ρ-1.2 Cu-150-160 g/L	• Does not remove Sn/Pb solder plating that covers the protected surface of copper circuit. • Used for outer circuit only. • Minimum undercut, high copper dissolving capacity, fast etch rates. • Regeneration is less hazardous.	• Being a chelator inhibits sodium hydroxide metal precipitation during waste treatment.

Spent ammoniacal etching solutions are alkaline solutions at a pH 8.5-9.5, having a typical copper concentration of 130-160g/l, a chloride concentration of 175-190 g/L and a molar ratio of ammonia to copper 4:1 with trace quantities of organic and/or inorganic chemical additives required for the etching process (Panias, 2002).

As the etching process proceeds and the copper concentration in the solution increases, the rate of etching gradually drops hence, a part of the solution has to be replaced with fresh etchant. During ammoniacal etching the copper concentration in the spent ammoniacal etching solution depends on the composition of the bath. Maximum etching efficiency is obtained when the ammoniacal solution contains 110-130 g/L copper and efficiency decreases drastically when the copper concentration is 150-170 g/L (Kyuchoukov *et al*., 1998). As more and more copper dissolves into etchant, the specific gravity of etchant increases, resulting in a lower etching speed. In order to keep the etching efficiency constant and optimal, the etching solution is continuously removed and regenerated. In order to achieve a stable etching operation, replenishment of fresh etchant is necessary.

Copper build up in the etch solution is accompanied with a corresponding depletion of the free ammonia content in the etch solution necessitating regeneration of the spent etch liquor. Ammoniacal etchant can be regenerated on site by recovering copper and recycling the etchant, simultaneously reducing the fresh etchant requirement as well as water discharge (Combs 2007). After copper removal, the etchant is regenerated by adding makeup solvent and ammonia is directly recirculated to the process (Fries, 1999). The other option is to send the solution back to the supplier who either reclaims the copper or regenerates and reformulates the solution and sends it back to the manufacturers, which satisfies a dual purpose of environmental sustenance and economics.

On large scale operations the commonly used methods for replenishing are crystallization, solvent extraction and electrolytic recovery (Keskitalo *et al*., 2007) have presented a comprehensive review on the different methods, electrowinning, cementation, solvent extraction, precipitation and membrane technology for the regeneration of acidic cupric chloride etchant waste along with their advantages and disadvantages. A critical analysis on the previously used, currently used and the future prospects in the regeneration technologies for etching solutions from PCB are reported by Yu *et al.* (2016).

The MECER process which is integrated with the production process uses solvent extraction and electrowinning to recover the etchant and reclaim high purity copper. In the MECER process, the copper concentration in the etching solution, which initially is 120-130 g/L, is reduced to 80-90 g/L by extraction and the raffinate is send back to the etching line. Copper is stripped with sulfuric acid and pure copper is produced by electrowinning. The process is applicable for rinse waters also where the copper content is reduced so as to discharge the waste waters in an environmentally friendly manner (Fries, 1999).

Almost 1.5–3.5 L of waste etchant is generated per square meter of PCB produced (Liu *et al.*, 2017). More than 70 thousand tons of copper goes in waste etching solution each year (Yu *et al.,* 2016). The total amount of copper discharged from the inner and outer layer etching process is approximately 93 percent of the total amount of copper discharged. The amount of copper discharged from the micro etch baths is approximately the same as the copper contained in the rinses. However, this varies for every printed circuit board factory (Avery and Moleux, 2007). Table 5.2 lists the different processes used to recover copper from both acidic and ammoniacal PCB etch solutions.

Copper from wastewaters of printed circuit boards can be reclaimed and utilized in a different fashion. Fouad and Basir, (2005) prepared ultrafine copper powders from PCB spent etch solutions using cementation technique. Liu *et al*. (2016) recycled hierarchical tripod-like CuCl from Cu-PCB waste etchant for lithium ion battery anode. Copper could be reclaimed as CuO and the resulting CuO powders were found to be suitable as raw materials in the synthesis of high-temperature superconductors, materials with giant magnetoresistance, magnetic storage media, catalysts, pigments, gas sensors, p-type semiconductor, and cathode materials, among others. (US 2017/0015836A1).

In India, particularly in the state of Gujarat, some of the major PCB manufacturers are located. Hence, recovery of copper from PCB etch solutions is very relevant to local business for environmental sustenance and it could yield fairly decent commercial benefit as well.

Table 5.2: Recovery methods for etching solutions and their operating parameters

Source	Recovery method	Composition of etchant	Operating Parameters	Reference
Synthetic spent copper (II) chloride etchant	Electrolytic	1.7M, $CuCl_2$, 0.1MCuCl, 2M HCl and 2M NaCl	Voltage-1.63 V, Power-1.54 kWh/kg (on-site regeneration and recovery)	Yang et.al. 2013
Ammonical spent copper etchant		30.8 g/L Cu, 2.09 M NH_3, 38.5 g/L chloride	pH -8.5 to 9.5, Agitation rates -255 to 123 min^{-1}, Current density-1100Am^{-1}, Cu recovery-99.8 to 99.9%	Giannopoulou et.al.2003
Spent etchant cupric chloride	Electrowinning	124 g/L Cu, 60 g/L HCl	Power-2.7 Wh/g, η-92%, Temp.-25-35^{0}C, Current density-0.16 to 0.3A/cm^2	Yaro and Hanna 2007
Spent nitric etching solutions		3.5 N HNO_3, 30g/L Cu, 40 g/L Sn, 40 g/L Pb, 20 g/L Fe	pH-2.1, Current- 3A Deposition time-20h, Cu recovery 98%	Lee et.al. 2003
Spent etchant	Membrane. electro-winning	167.8 g/L Cu, 158.6g/L Cl, 3.9 g/L carbonate, 5.3 g/L phosphate, 0.5 g/L thiourea	Temp. 40-50 ^{0}C, current density 500-1500 Am^{-1}, cell voltage 2-2.5 V, Cu recovery-90.00%	De-liang and Ren-hua 2005
Spent etchant	Supported liquid membrane	Cu, 2.5M ,NH_3, 10M, Cl-,5M, pH 10	Polypropylene membrane, Surface area 1.4 m^2, 33%v LIX 54	Yang and Kocherginsky 2006
PCB spent etching solution	Ultrasonic	114.1 g/L Cu	Power-300W, Stirring rate -300rpm, Cu recovery-93.76%	Huang et.al. 2011
Acid Cu-PCB waste etchant	Liquid chemical reduction	95 g/L Cu	Time -12h, pH-3, CuCl recovery-85%	Liu et.al. 2016
Ammonical spent copper etchant	Cementation	135 g/L copper	Temp.-25^{0}C, Time-20 min, pH 2, Purity of Cu>99%	Fouad and Basir 2005
Synthetic ammonium chloride etchant	Solvent extraction	Cu 0.01M, ammonium chloride 5 M	Extractant-Pyridineketoximes 0.01 to 0.2M), pH - 9 Stripping agent- water, Cu recovery 80–90%	Wieszczycka et.al. 2012
		Cu 112.98 g, 6M NH_3	Extractant- 40% hindered β-diketone, O/A- 5/4 H_2SO_4 stripping, O/A- 1:2, Cu recovery 98.27%	Qi-wen et.al. 2011
PCB spent etchant		Cu 152.1 g/L	Extractant- 40% LIX54, O/A-5/1, H_2SO_4 stripping, O/A- 2.5/1, Cu recovery 54%	Sze and Wong 1994

5.5 Experimental

The metals present and their content in the etch solution was determined using ICP-OES. The ammoniacal nitrogen, chloride, sulphate and nitrate content in the etch solution were also determined by methods discussed in Chapter 3.

5.5.1 Extraction

Copper extraction from etch solution was carried out using LIX 84-I in kerosene by contacting equal volumes (100 ml each) of the organic and aqueous phases in shake flasks on a rotary shaker (Remi-RS 24BL) at 150 rpm and 30^0C. The effect of equilibrium pH on the extraction of copper was studied using 20% (v/v) LIX 84-I at pH values ranging from 8.5 to 10. The effect of extractant concentration was studied by contacting the etch solution with organic phase containing 10% (v/v) to 50% (v/v) LIX 84-I in kerosene. To determine the number of stages required for extraction, the etch solution was equilibrated with 20% (v/v)LIX 84-I as well as 50%(v/v) of LIX 84-I at varying organic to aqueous phase ratios. The aqueous phase metal concentration was determined using AAS discussed in Chapter 3.

5.5.2 Precipitation-Stripping

After extraction the organic phase was separated and scrubbed with water. Stripping was carried out by contacting the loaded organic phase with an equal volume of 1.0 M oxalic acid solution for time intervals ranging from 15 minutes to 3 hours on a rotary shaker (Remi-RS 24BL) at 30 ± 2^0C and 150 rpm. Stripping was also carried out using 1.0 M oxalic acid prepared in ethanol-water mixtures containing 10% to 50% ethanol by volume. After the stipulated stripping time the aqueous and organic phase were separated. Copper oxalate precipitate in the aqueous phase was centrifugally separated, washed and dried. Decomposition pattern of copper oxalate to copper oxide was investigated using TGAanalysis and the temperature of decomposition was discerned. The oxalate precipitates formed were calcined in a tube furnace at 400^0C for 3 hours to obtain copper oxide.

5.5.3 Characterization

Particles formed were characterized for their material properties by XRD and FTIR, morphology by FESEM, surface characterization by zeta potential and size distribution using laser diffraction. Surface area of the oxide particles was measured by BET techniques. All these analysis were carried out as per operating procedures mentioned in Chapter 3.

5.5.4 Catalytic activity

Materials

- Nitrobenzene: Nitrobenzene of AR grade with assay 99% supplied by Spectrochem Pvt. Ltd. Mumbai was used as a reagent for the production of aniline.
- Methanol: Methanol of AR grade with assay 99% was supplied by S.D.fine Chemical limited used as a solvent for the production of aniline.
- Sodium borohydride: Sodium borohydride ($NaBH_4$) of assay minimum 97% was used as a reducing agent for reaction of nitrobenzene to aniline.
- Sodium chloride: Brine solution (saturated NaCl solution) helps to disrupt any emulsion formed during synthesis and dry the organic layer by extracting water that may have dissolved in the organic phase.
- Sodium sulfate: Anhydrous sodium sulfate (Na_2SO_4) was used to bind any water remaining in the organic solution and also act as a drying agent during production of aniline.
- Petroleum ether: Petroleum ether of assay minimum 90% v/v of Merck Specialties Private Limited was used as carrier for Thin Layer Chromatography (TLC).
- Ethyl acetate: Extra pure ethyl acetate of S.D Fine Chemicals Limited was used as carrier for TLC and as a solvent for Gas Chromatography (GC).

Method

Copper oxide particles obtained were used to catalyse the reduction reaction of nitrobenzene to aniline using methanol as a solvent. A mixture of nitrobenzene, copper oxide and solvent methanol were added to a three-necked flask, and sodium borohydride was added drop wise to the above solution under continuous stirring. The mixture was stirred and progress of reaction was monitored by TLC. After the completion of reaction, the mixture was cooled to room temperature, filtered, and the catalyst was separated. The filtrate was washed with methylene chloride and further with brine. This led to the formation of two layers. The organic layer containing the product was washed with water. Further, anhydrous Na_2SO_4, was added and the solvent was removed under vacuum. The product formed was analysed on a gas chromatograph. From the area under the curve obtained the concentration of the species present was evaluated.

5.6 Results and Discussion: Copper extraction

Recovery of copper from ammoniacal solutions is important in various hydrometallurgical processes. Solvent extraction is by far the most widely used method to recover copper from ammoniacal solutions due to its inherent advantages; ease of operation; low energy requirement and can handle a wide range of feed concentration (Kyuchoukov *et.al.,* 1998). β diketones and hydroxyoximes are the most widely used extractants to recover copper from ammoniacal solutions (Hu et.al. 2012). LIX 63 that was introduced in 1963 was used to extract copper from ammoniacal leach solutions which was later supplemented by LIX 65N and still later by LIX 84-I (MCT Redbook).

A number of workers studied copper extraction from ammoniacal solutions using different extractants viz. the hydroxyoxime LIX 84-I was used by Rosinda et.al. (2002), Sengupta et al. (2007, 2009), Lurdes et al. (2010), Ochromowicz et al. (2014), Wang et al. (2017). The strong copper extractant LIX 984 N was also studied by Ochromowicz et al. (2014). The β diketone LIX 54 was used by Kyuchoukov et al (1998), Algucil and Alonso (1999), Rosinda et al. (2004), Ochromowicz et al. (2014). Sterically hindered β diketone was used by Liang et al. (2011). Current status and the future perspective of recycling by hydrometallurgical routes are detailed by Xu *et al.* (2016).

Spent etchant solution collected from a small scale PCB manufacturing unit in Baroda manufacturing 500 m^2/ month had a pH of 8.5. The metal composition determined of the by ICP analysis and chloride, sulfate, nitrate and ammoniacal nitrogen content were determined using APHA techniques is given in Table 5.3.

Table 5.3: Composition of spent printed circuit board etchant

Component	Concentration (mg/l)
Copper	51800
Nickel	3.375
Lead	33.535
Zinc	14.05
Tin	1.856
Ammoniacal Nitrogen	48675
Chloride	53853
Sulfate	395
% of Ammonia	5.90
pH	8.5
Specific gravity	1.307

5.6.1 Copper speciation in ammoniacal media

The spent etchant from the ammoniacal etching process contained ammoniacal nitrogen. Ammonia acts as a molecular ligand for the formation of stable ammine copper (II) complexes. (Giannopoulou *et al.,* 2003). In ammoniacal solutions hydrated copper reacts with ammonia to form various copper ammine species. The coordination number of hydrated copper (II) species decreases when the coordinated water is replaced by ammonia. The geometry of the specie changes from octahedraon to distorted planar square when the water of hydrated copper is replaced by two or more ammonia molecules, similarly with an increase in the aqueous phase pH the copper (II) species changes from axially elongated octahedron to distorted planar square (Hu *et al.,* 2013). Copper extraction is sensitive to the presence of copper ammine species in the aqueous phase (Hu *et al.,* 2012).

The species distribution diagram of copper (II) ions for the spent etch solutions as a function of solution pH was plotted using *Visual MINTEQ 3.1* (Figure 5.3).

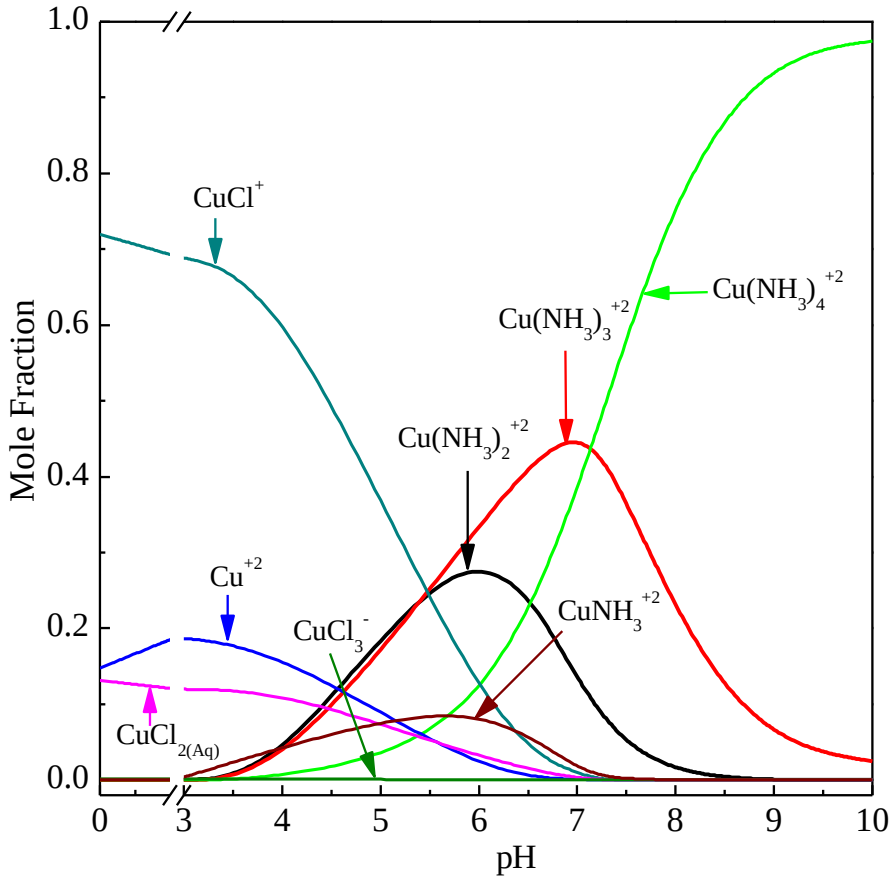

Fig.5.3: Speciation diagram of copper species present in PCB etch solution as a function of pH

From Figure 5.3 it was found that the ammine copper (II) complex, ($Cu(NH_3)_4^{2+}$), absolutely dominates from pH 2 to 10. Among these complex ions, the tetraammine copper (II) complex ion,($Cu(NH_3)_4^{2+}$) is the most important, having a broad stability area extended from pH 4 to pH 10. At a pH value of 8.5, that of spent etchant collected from printed circuit board manufacturing unit, copper is predominantly present as $Cu(NH_3)_4^{2+}$. Rosinda *et al.* (2004) reported that Cu complex with four NH_3 is the dominant form present in ammoniacal solutions having excess of NH_3 to copper. Such predominance of $Cu(NH_3)_4^{2+}$species is expected due to its high formation equilibrium constant over other ammine complexes.

5.6.2 Copper extraction from ammoniacal solution:

Solvent extraction (SX) of copper (II) from ammonia solutions proceeds similar to that from acidic solutions, but complexation of metal by ammonia ligands must be considered (Ochromowicz et.al.2014). During extraction ammonia ligands are pushed out and a new chelate complex with hydroxyoxime is formed in organic phase. The mechanism of copper extraction from ammoniacal solutions using hydroxyoximes and β diketones based on existence of $Cu(NH_3)_4^{2+}$ species in the feed can be described by Equation 5.8 (Kyuchoukov *et al.,* 1998).

$$Cu(NH_3)_4^{2+} + 2HR \leftrightarrow CuR_2 + 2NH_4^+ + 2NH_3 \quad (5.8)$$

where HR represents the extractant and CuR_2 the copper-extractant complex.

5.6.3 Effect of equilibrium pH

Copper extraction was carried out using LIX84-I at equilibrium pH values ranging from 8.5 to 10 using 20% (v/v) LIX84-I at equal O/A ratios. It was observed that percentage extraction increased from 20.66 % at pH 8.5 to 22.01% at pH 8.9 and thereafter decreased to 20.27 % at pH 10 (Figure 5.4). Alguacil and Alonso (1999) also reported highest extraction efficiency in pH range of 7-9, while Rosinda *et.al.,* (2010) observed maximum extraction efficiency in the pH range 8-10, above this pH they found a sharp decrease in the amount of copper extracted and attributed this to the corresponding increase in the ammonia concentration. Rice and Nedved (1978) reported increasing pH and free ammonia concentration decreased the fraction of uncomplexed metal in the aqueous phase resulting in decrease of metal extracted.

Equation 5.8 shows that there is an increase in ammonia concentration due to release of ammonia leading to an increase in the pH. Nathsharma and Bhaskarsharma (1993) reported that in actual practice there is no increase in pH due to buffering by ammonium ion, rather there is a small decrease due to uptake of ammonia in the organic phase. Though hydroxyoximes have a high affinity for copper they also have a tendency to co-extract ammonia. Hydroxyoximes transfer ammonia especially at higher (pH >9) due to the presence of nonyl phenol in the extractant (Lurdes *et al.*, 2010) resulting in decrease in the extraction. The increased stability of the ammine complexes also inhibits extraction and copper extraction decreases as the copper (II) species with distorted configuration increases due to an increase in pH.

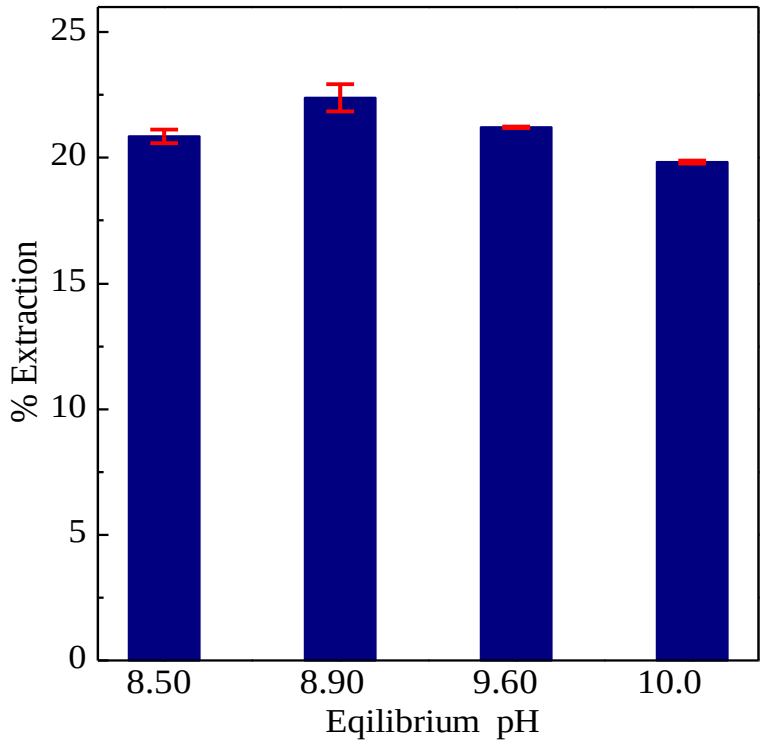

Fig. 5.4: Effect of equilibrium pH on percentage extraction (LIX 84-I=20% (v/v), O/A= 1)

5.6.4 Effect of extractant concentration

Experiments were carried out at varying extractant concentrations ranging from 10% to 50% (v/v) LIX 84-I at O/A ratio 1 and an equilibrium pH of 8.9 to investigate the effect of extractant concentration on the extraction of copper. It was observed that increase in extractant concentration from 10% to 50 % resulted in an increase in the percent copper extraction from 13.38% to 51.54 % in a single stage (Figure 5.5).

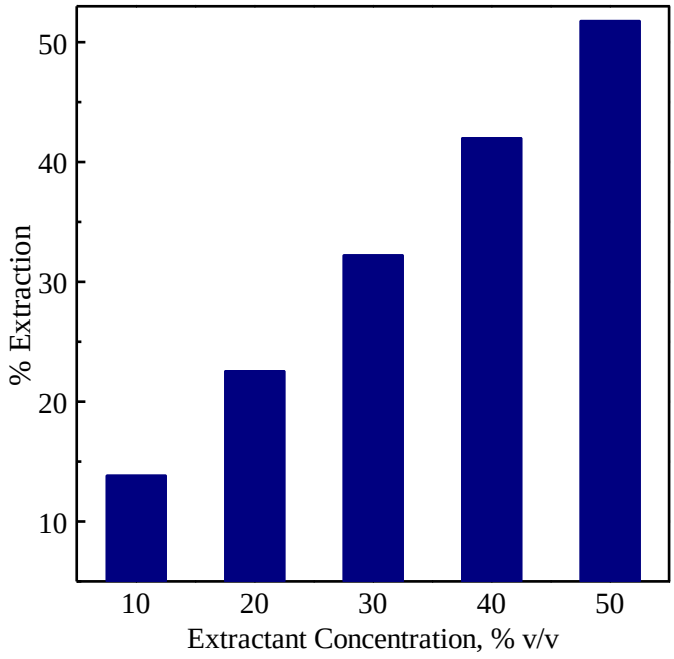

Fig. 5.5: Effect of LIX 84-I concentration on % extraction (pH=8.9, O/A=1)

5.6.5 Extraction isotherm and counter current simulation

Isotherms are unique to the conditions under which they are generated. If even one of the parameter is changed, say for example reagent concentration then the copper concentration of the respective organic or aqueous phase changes and a different isotherm gets generated. A properly generated extraction isotherm represents equilibrium conditions and it predicts the best extraction which can be obtained. These isotherms can be used to set the staging in the circuit.

Maximum copper extracted for a given O/A ratio is obtained from the extraction isotherm. To determine the phase ratio and the number of stages required for extraction the spent solution was equilibrated using 20% (v/v) LIX84-I at O/A phase ratio ranging from 1:6 to 6:1 and 50% (v/v) LIX 84-I extractant concentration at O/A phase ratio ranging from 1:3 to 2:1. McCabe–Thiele plots indicate that three stages are required for complete extraction of copper at a phase ratio of 4.5:1 using 20% (v/v) extractant and 1.5:1 at an extractant concentration of 50% (v/v) (Figure 5.6).

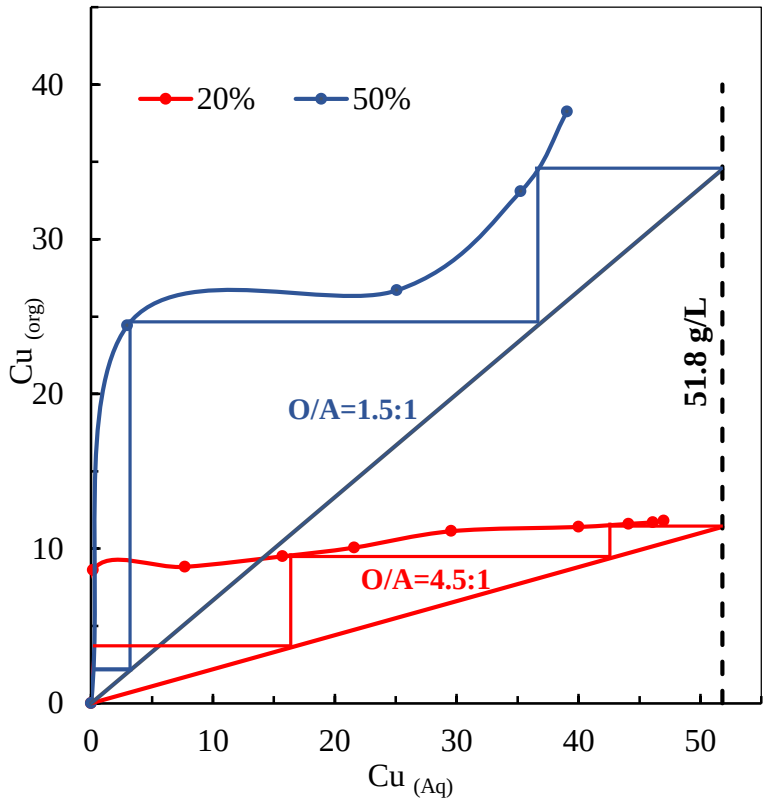

Fig. 5.6: McCabe –Thiele plot for copper extraction using LIX 84-I at varying extractant concentrations

Based on the McCabe–Thiele plots, a three-stage counter-current simulation study was carried out at phase ratio (O/A) 4.5:1 for 20% (v/v) LIX 84-I and at 1.5:1 for 50% (v/v) LIX 84-I. The results indicate a loading of 51.79 g/l copper in the organic phase corresponding to total copper extraction of 99.9% in both cases with 3 mg/L and 5mg/L of copper in the raffinate from the third stage for 20% and 50% (v/v) LIX 84-I concentration respectively (Figure 5.7a, Figure 5.b).

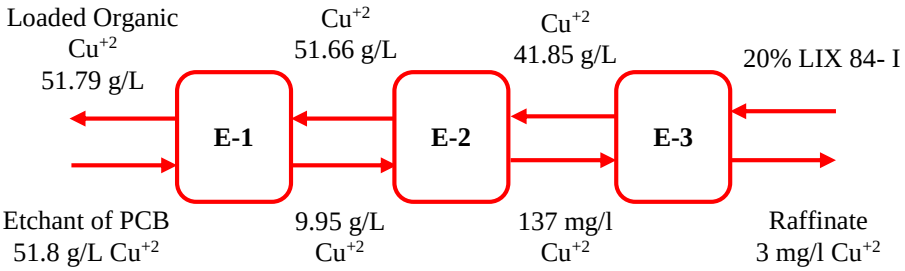

Fig.5.7a: Counter-current simulation for copper extraction using LIX 84-I=20% (v/v), O/A =4.5:1

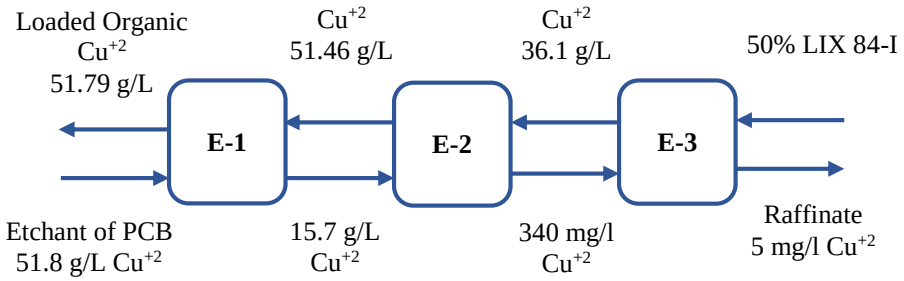

Fig.5.7b: Counter-current simulation for copper extraction using LIX 84-I= 50% (v/v), O/A =1.5:1

5.7 Result and Discussion: Precipitation-Stripping of copper

The organic phase containing 50% (v/v) LIX 84-I was loaded with 26.7 g/L of copper on contact with the etch solution at equilibrium pH of 8.9 and O/A ratio of 1 accounting for the 51.4% of copper extracted from the etch solution. The organic phase after extraction was washed with water several times to remove the adhering ammonia prior to stripping. Copper was stripped from the organic phase by contacting with an aqueous oxalic acid solution that led to the precipitation of copper oxalate. The total copper stripped from organic phase is the sum of copper present in the precipitate and the copper remaining dissolved in the oxalic acid solution.

5.7.1 Precipitation-Stripping of copper using oxalic acid solutions

Stripping was performed at equal O/A ratios by contacting the organic phase loaded with 26.7 g/L of copper using 1M oxalic acid. The percent copper stripped as copper oxalate with time is shown in Figure 5.8a. The amount of copper oxalate stripped increased with an increase in contact time. After one hr of stripping time,77.4% of the loaded copper was stripped and precipitated as copper oxalate and thereafter no further precipitation-stripping occurred (Figure 5.8(a)) necessitating a second contact of the organic phase with fresh acid.

The oil phase was further contacted with 1M oxalic acid to strip the residual copper present after the first stage. Hence, the amount of copper stripped in first stage was 20.67 gm in a first stage and 5.84 gm in the second stage.

Experimental data show that out of the 26.7 gm copper loaded in the organic phase, the amount of copper precipitated as oxalate was 20.55 gm in first contact, subsequently contacting the organic phase again with fresh acid resulted in precipitation of 5.77 gm of oxalate accounting for a cumulative copper oxalate precipitate yield of 98.57%. Copper remaining soluble in oxalic acid after precipitation was determined AAS. It was found that the soluble copper was 0.12 gm and 0.07 gm after the first and second contact respectively. Thus, net copper stripped in first contact from organic phase turns out to be 20.67 gm indicating that percent copper precipitated in first contact from the total amount stripped is 99.42%, while for the second contact it turns out to be 98.8%.

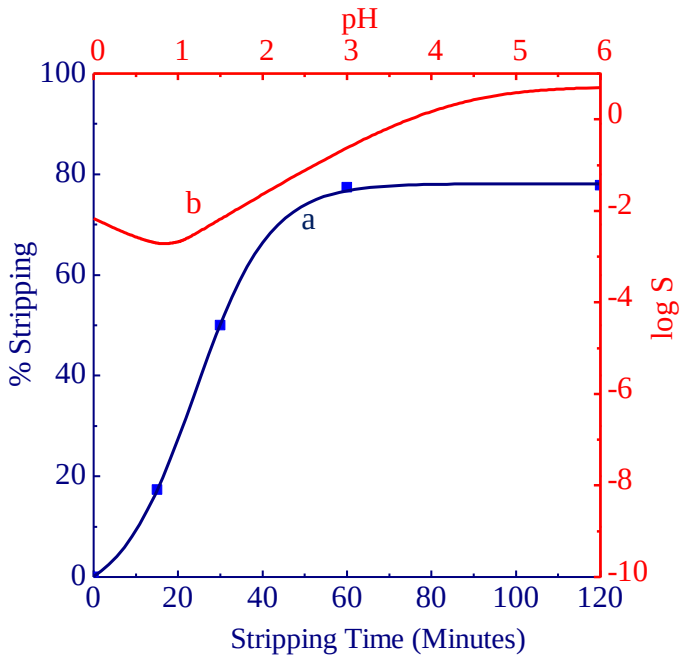

Fig. 5.8: (a) Effect of stripping time on percentage stripping of copper (b) Copper oxalate solubility curve.

Based on theoretical considerations using the solubility diagram developed in this study and the sequence of calculations elucidated in Section 4.6.11, it could be predicted that copper solubilized in the first contact, at precipitation pH value of 0.85 (Fig. 5.8 (b)), was 0.075 gm while in the second contact it was 0.034 gm indicating copper precipitated from net copper stripped in the first contact was 99.64% and in the second contact it was 99.41%. Thus the experimental and predicted values are in very close agreement as shown in Table 5.4 indicating the robustness of the calculation procedure.

5.7.2 Precipitation-stripping of copper in ethanol-oxalic acid mixtures:

Copper oxalate particles obtained by precipitation stripping of the copper loaded organic phase were observed to be highly agglomerated and clustered Figure 5.12. In literature it is reported that agglomeration of particles decrease substantially in presence of alcohol, Ran *et al*. (2006) observed that copper oxalate precipitation in ethanol/water solution reduced particle agglomeration considerably. Ethanol as solvent was used by (Ciantti, 1983; Qui *et al*., 1999) to form water-in-oil microemulsions for preventing particle agglomeration. Zhang *et al*. (2009) used 50%v/v of ethanol as the stripping phase to prepare copper oxalate powders using stripping-precipitation process.

Precipitation stripping of copper was also performed using ethanolic solutions of oxalic acid to explore the possibility of obtaining less agglomerated and uniform size oxalate particles. The amount of ethanol in the aqueous solution was varied in the range from 10% to 50% with oxalic acid concentration 1M in all samples. Table 5.4 shows the experimental results for precipitation- stripping and those predicted from theoretical considerations. It can be seen that presence of alcohol resulted in a higher percentage of recovery of copper oxalate. Increase in ethanol content in the ethanolic oxalic acid mixture increased the yield of oxalate particles. With 25% and higher amount of ethanolic oxalic acid, precipitation of copper oxalate was achieved in a single stage which was equivalent to the precipitation and recovery of oxalate particles obtained in two stages when stripped with aqueous oxalic acid solutions.

Table 5.4: Stage wise recovery of copper

Stripping solution	Sample	Stage	Copper loaded 26.7 gm						
			Amount(gm)					% Yield	
			S	Experimental		Predicted		E	T
				Sl	P	Sl	P		
Oxalic acid	AQ	1	20.67	0.12	20.55	0.075	20.6	99.4	99.6
		2	5.84	0.07	5.77	0.034	5.8	98.8	99.4
10% ethanol-oxalic acid	E(10)	1	21.99	0.1	21.89	0.06	21.95	99.54	99.81
		2	4.57	0.05	4.5	0.02	4.54	98.91	99.34
25% ethanol-oxalic acid	E(25)	1	26.25	0.084	26.16	0.049	26.2	99.68	99.86
50% ethanol-oxalic acid	E(50)	1	26.27	0.072	26.2	0.036	26.23	99.73	99.86

S: Stripped, P: Precipitated, E: Experimental, T:Theoretical, Sl: soluble

The amount of oxalate remaining dissolved in the stripping solution was determined experimentally and also predicted based on theoretical considerations. The required solubility diagram was developed using the method detailed in Chapter 4 except that $log\ K_1$, $log\ K_2$ and $log\ K_{SP}$ values (Cyrille *et al.*, 2014) used were for the ethanolic oxalic acid solutions as shown in Table 5.5.

Table 5.5: Key solution properties of strippants

Sample	pH	$log\ K_1$	$log\ K_2$	Solubility product ($log\ K_{SP}$)	Dielectic constant**	Surface tension (mN/m)	Interfacial tension* (mN/m)
AQ	0.84	-4.26	-1.25	-9.14	76.75	51.5	15.7
E(10)	0.9	-4.6	-1.5	-9.099	72.15	45	11.6
E(25)	0.94	-5.15	-1.8	-9.048	65.22	34.9	5.8
E(50)	1.3	-6.05	-2.35	-9.032	51.91	29.4	2.3

*with kerosene containing 50%(v/v) LIX 84-I
** (Wyman, 1931)

Figure 5.9 shows the solubility curves developed based on the theoretical conditions. The theoretical values of solubility reported in Table 5.4 are evaluated from the solubility diagram at the precipitation pH. It can be seen that the dissolved oxalate in ethanolic solution was lower than that obtained while stripping with aqueous oxalic acid solutions.

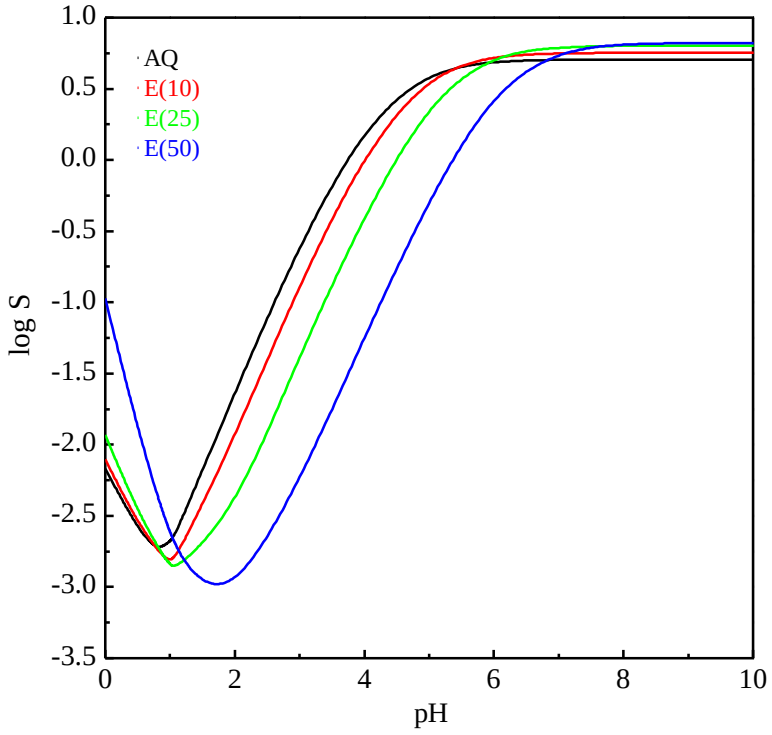

Fig. 5.9: Copper oxalate solubility in ethanolic oxalic acid solutions

This is attributed to the lowering of the solubility product of the copper oxalate in ethanolic oxalic acid solution (Table 5.5). Metal oxalates are almost insoluble in pure alcohol and the solubility of the oxalate in a mixed alcohol/water solvent will be lower than in pure water.

In ethanolic solutions the ionisation of oxalic acid is reduced because of lower dielectric constant compared to that of water. Hence, the ionisation reaction of $H_2C_2O_4$ to $H^+$and $H_2C_2O_4$ (Equation 4.11) will be slow. The decrease in dielectric constant with increasing nonpolar solvent concentration causes the solubility to decrease. The solubility curves obtained (Figure 5.9) show highest solubility of oxalate in aqueous oxalic acid solutions and a low solubility in 50% ethanolic oxalic acid solutions. The reduction in ionization of oxalic acid in presence of ethanol causes a corresponding reduction in H^+ ions in the system, which would result in the decline of stripping rate as well as the rate of precipitation of the copper oxalate. However, contrary behavior was observed and rates of precipitation are substantially increased in the presence of alcohol.

The precipitation – stripping environment in ethanolic oxalic acid solution is quite complex involving multiple interactions and effects viz.

(i) Presence of ethanol results in lowering of interfacial tension between oil and the aqueous phase (Table 5.5) leading to formation of fine dispersions on agitation

(ii) Solubilisation of oil in alcohol further leads to the stability of the dispersion. Alcohol (ethanol) molecule has both polar and nonpolar parts, unlike water, which is highly polar and oil (kerosene) which is completely nonpolar. Hence, in absence of any form of charge on them to cause repulsion, oil gets solubilized in ethanol. However, the amount of oil that will dissolve depends on whether there is more water or alcohol to the mixture. When ethanolic solution fails to dissolve oil, it forms a dispersion of oil globules.

(iii) Precipitation of the oxalate particles and their presence at the interface leads to further stabilization of the dispersion. The combined effects of all these factors override the decline in precipitation rates expected due to the reduction of ionization of oxalic acid.This leads to rapid stripping of copper from oil phase due to the enormous increase in the surface area caused by the formation of oil- water dispersion in comparison to the area generated on a shaker. Hence, the stripping process gets completed in a single stage contact and in less time. However, the complexity of the situation inhibits us from identifying effects of individual factors at this juncture.

Figure 5.10 shows the conditions during stripping at 30 mins for the four samples. The dispersions formed at varying ethanol content during stripping are clearly visible.

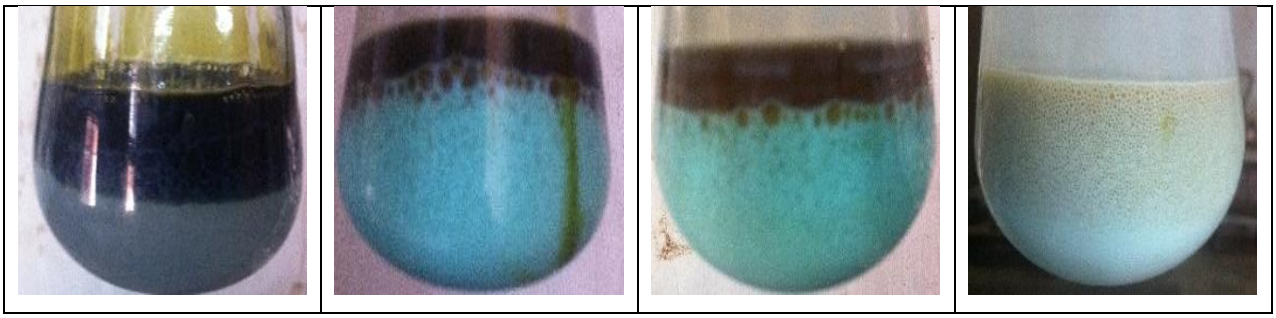

AQ E(10) E(25) E(50)

Fig. 5.10: Dispersion formed during agitation

The distribution of the soluble copper species in the aqueous phase for all the four samples was theoretically predicted form the solubility calculations as discussed in Chapter 4. With an increase in the ethanol content of the stripping solution, equilibrium pH values after stripping also increased (Table 5.5), as less H^+ions were available in solution because of low ionisation constants in ethanolic solutions. These H^+ ions bind with soluble copper to form $CuHC_2O_4$. Hence, percentage of $CuHC_2O_4$ soluble species is more in solutions stripped with aqueous solutions of oxalic acid (Figure 5.11a). On increasing the ethanol concentration the free H^+ ions produced from oxalic acid are not available to bind with copper and hence Cu^{+2} species increase as the concentration of ethanol increases (Figure 5.11 b,c,d).

The oxalate powders obtained as a result of PS in oxalic acid and ethanol oxalic acid

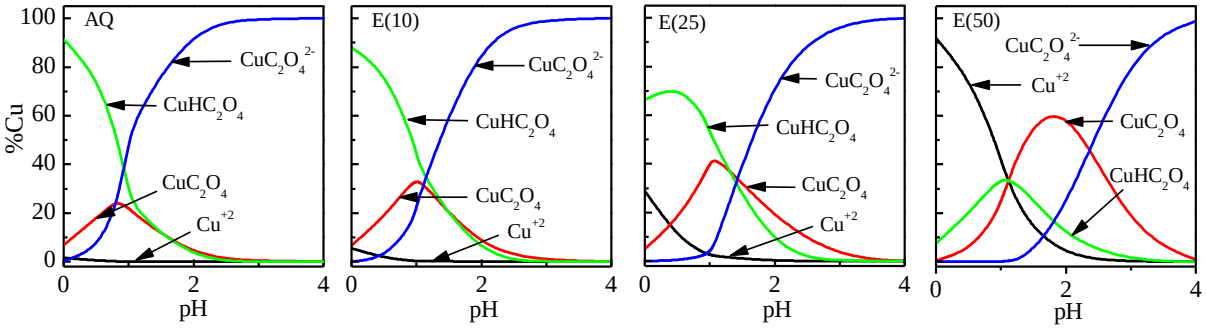

(a) (b) (c) (d)

Fig. 5.11: Soluble specie distribution curves of copper- ethanolic oxalic acid solutions

solutions are shown in Figure 5.12. It can be observed that the clustering and agglomeration among the particles is substantially reduced and free flowing powders were obtained when stripping is carried out in presence of ethanol. Reduction in aggregation and agglomeration

of particles precipitated in ethanolic oxalic acid solutions is attributed to the lower surface tension of ethanolic solutions (Table 5.5) which causes low particle packing during drying (Winnubst et al., 2010).

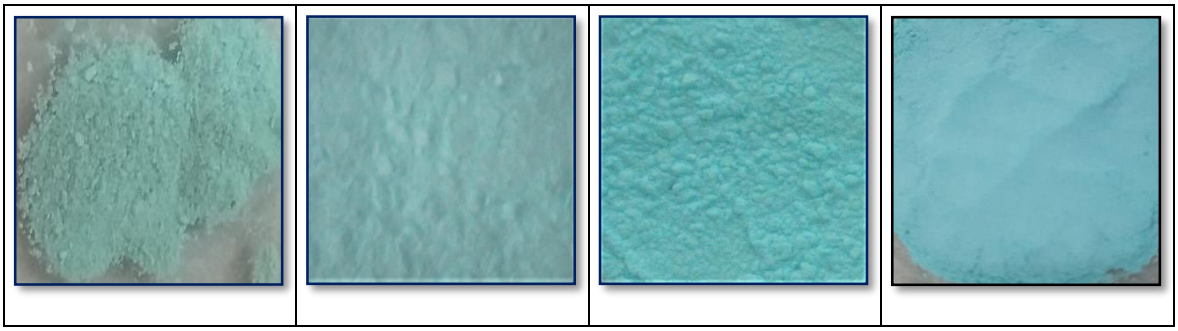

Fig. 5.12: Copper oxalate precipitate obtained from different stripping solutions

5.8 Results and Discussion: Characterization

The characterization of precipitated copper oxalate particles and the calcined copper oxide particles are detailed in this section.

5.8.1 Characterization of copper oxalate particles

The precipitates of copper oxalate obtained were characterised by XRD, FTIR, and their morphology was observed by FESEM. The particle size distribution and the zeta potential of the particles were evaluated. Thermogravimetric analysis was used to determine the thermal decomposition behavior of the particles. Sample preparation, procedure for the measurements and the details of the instruments used for characterization are reported in Chapter 3.

X-Ray Diffraction analysis

Figure 5.13 shows the XRD patterns of copper oxalate for samples AQ, E(10) and E(50). The sharp diffraction peaks of copper oxalate particles precipitated using oxalic acid solutions and ethanolic solutions containing 10% and 50% ethanol could be assigned to the (110), (120), (011), (111), (220), (121) and (130) planes of orthorhombic copper oxalate that matched with standard data JCPDS 21-297 and those reported in literature for synthesis of copper oxalate using oxalic acid. (Jongen *et al.*, 2000) No characteristic peaks of other materials were detected, indicating the high purity of the copper oxalate formed.

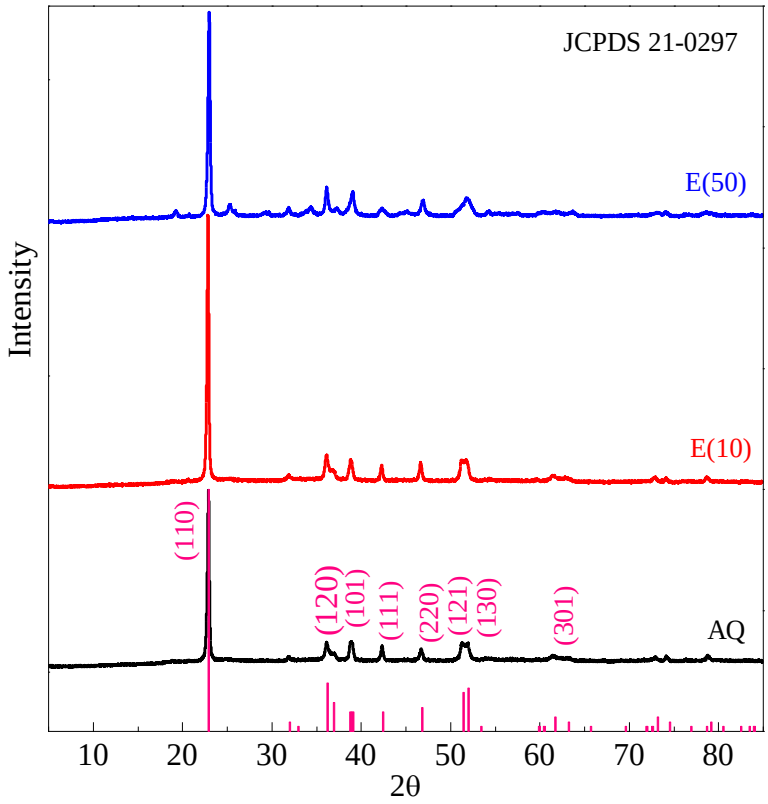

Fig. 5.13: XRD of copper oxalate

The crystallite size (d) calculated using Debye–Scherrer formula is shown in Table 5.6 Increasing the percentage of ethanol in the ethanolic oxalic acid solutions resulted in a decrease in the crystallite size. The crystalline structure of the copper oxalate is the Pnnm space group with the lattice parameters as shown in Table 5.6.

Table 5.6: Crystallite size and lattice parameters for copper oxalate

Sample	Crystallite size (nm)	Lattice parameter		
		a (Å)	b (Å)	c (Å)
AQ	27.5	5.37	5.91	2.54
E(10)	23	5.39	5.60	2.55
E(50)	16.6	5.32	5.60	2.54

Fourier transform infrared spectroscopy

IR spectra, Figure 5.14, of copper oxalate for sample AQ, E(10) and E(50) show a broad band at ~3430 cm^{-1} corresponding to the OH stretching vibration and the hydrogen bonds between the water molecules and the carboxylate group. A shift in the band attributed to the main antisymmetric carbonyl stretching band specific to the oxalate family from 1683 cm^{-1} to 1654.75 cm^{-1} is a pointer towards less amount of water in the particles precipitated in 50% ethanolic oxalic acid solution. Both these bands arise from the remaining water in the structure of the particles during precipitation (Rahimi-Nasrabadi *et al.*, 2013). Bands at 1363.48 cm^{-1} and 1320.07cm^{-1} correspond to $\sigma_s(C-O)+\sigma C-C)$ and $\sigma_s(C-O)+\delta O-C=O)$ respectively. Bands at ~824.1 cm^{-1} are due to $\delta(O-C=O)$ and 507.48 cm^{-1} are for the $\delta(Cu-O)$ for the oxalate moiety. Intensity of all the bands reduced as the alcohol concentration in the ethanolic oxalic acid solutions increased (Thakur and Joshi, 2012).

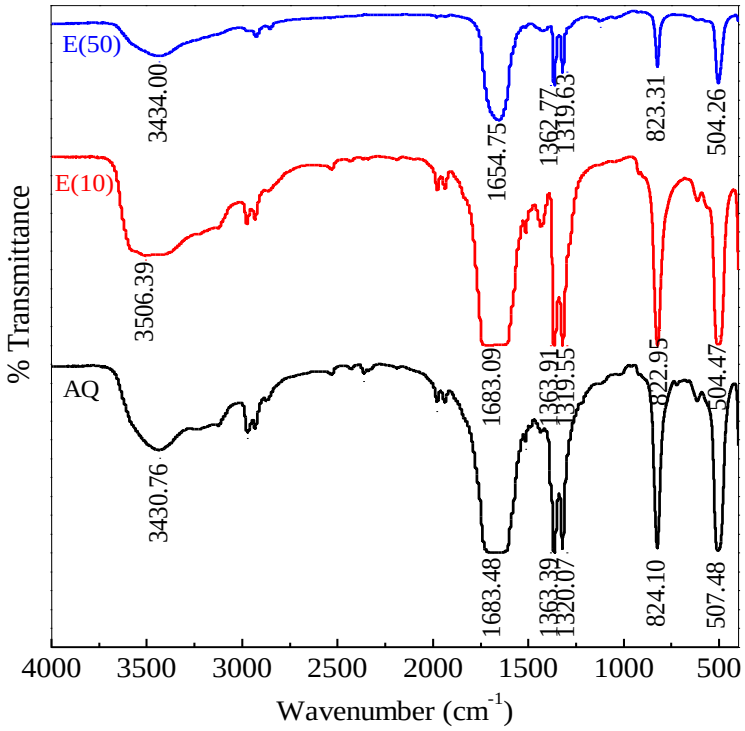

Fig. 5.14: FTIR spectra of copper oxalate

Particle morphology and size

The PS of copper loaded oil phase using 1M aqueous oxalic acid could be completed in two stages while using 1 M oxalic acid in 25% and 50% ethanolic oxalic acid solutions it was attained in a single stage. Precipitation was complete in one hr time duration. In precipitation

from aqueous oxalic acid solutions 77.8% yield of the copper loaded as copper oxalate particles was obtained in 1 hour while the yields with 10%, 25% and 50% ethanolic oxalic acid solutions was 82%, 98% and 98.5 % respectively. Hence, it was anticipated that in 1 hr precipitation time a stable particle size distribution would have been attained in all the three cases. Figure 5.15 shows the particle size distribution for three systems AQ, E(10) and E(50). It can be seen that the particles are small in size and the total distribution was spread over two orders of magnitude.

The particle size distribution of the precipitates formed in aqueous oxalic acid was wide with size range from 300 nm to 20 μm. The size distribution of the oxalate precipitated in 10% ethanolic oxalic acid solutions was even wider with size ranging from 100 nm to 20 μm. However, the shift towards lower sizes in ethanolic solutions is distinct in the size distribution. Agglomeration tendencies are also distinct in particle precipitated in aqueous media and E(10) ethanolic media.

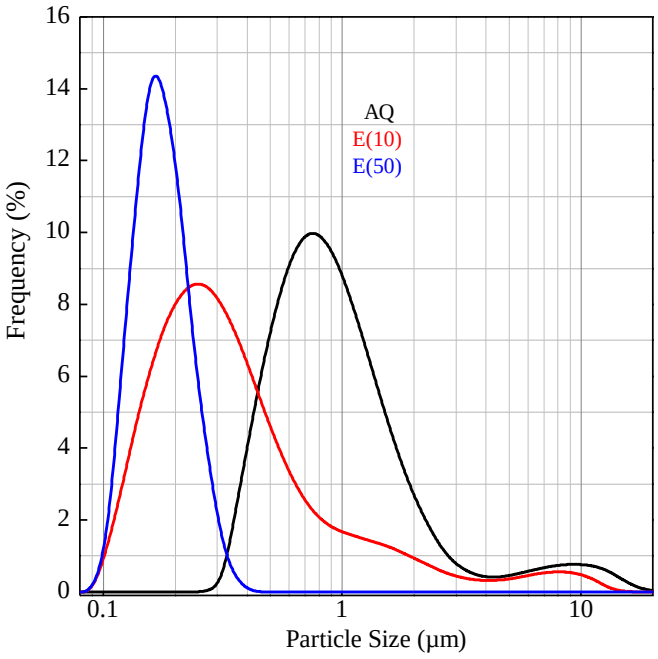

Fig. 5.15: Particle size distribution of copper oxalate

Narrow particle size distribution and submicron size particles were obtained when the oxalates were precipitated in 50% ethanolic oxalic acid solutions. Uniformity of size distribution is achieved through a short nucleation period that generates all the particles seen at the end of the precipitation process followed by self-sharpening growth process where

smaller particles grow more rapidly than larger ones and narrow particle size distribution is observed (Wang *et al.,* 2003). The decrease in the agglomerates is attributed to the lower surface tension in 50% ethanol oxalic acid solutions compared to oxalic acid solutions.

The significant parameters of the distribution are shown below. It is seen from the data that the statistics of the distributions is significantly affected by the presence of ethanol in the precipitating media.

Sample	D[3 2]	D[4 3]	D[0.1]	D[0.5]	D[0.9]
AQ	0.9	1.53	0.51	0.96	2.43
E(10)	0.303	0.788	0.16	0.32	1.41
E(50)	0.23	2.12	0.141	0.205	1.28

Polarity of the precipitating media influences the characteristics of the particles. A polar solvent leads to a formation of few nuclei which grow rapidly while in non-polar solvents there is formation of large number of small nuclei whose growth is inhibited leading to smaller size particles. Water being a polar solvent leads to the formation of few nuclei that grow rapidly resulting in larger size particles and wide size distribution. Addition of ethanol to the precipitating media lowers the polarity of the solution and alters the thermodynamics and nucleation kinetics (Chen *et al.,* 2004) as a result we get smaller size particles and also narrower particle size distribution.

The addition of ethanol results in a decrease in the dielectric constant of the aqueous solution (Table 5.5), the low value of the dielectric constant increases the supersaturation resulting in formation of homogeneous nuclei and smaller particles. Similar results were reported by Hu *et al.* (2012) who obtained submicrometer ZrO_2 powders in alcohol/water mixed solutions. They found that the dielectric property of the mixed alcohol/water solvent affected the nucleation and growth of zirconia particles. The slightly higher solubility of copper oxalate in water in comparison to that in ethanol solutions resulted in fast particle growth via Ostwald ripening which lead to the formation of pimary particles of larger size and greater aggregation. (Xiu *et al.,*2008).

Zeta (ζ) potential

Zeta potential measurements provide insight into the stability of particulate suspensions. Surface properties primarily determine the agglomeration state where the particles are held

by weak Van der Waals forces. Zeta potential of the copper oxalate particles precipitated in the aqueous oxalic acid solutions and ethanolic oxalic acid solutions were measured using Malvern Zetasizer. The dispersion media was water at a pH of 6.8. Samples were sonicated externally for 20 min, to disperse the agglomerates, prior to measurement. All the particles showed negative surface charge with a value of -34.29 mV for particles precipitated in aqueous oxalic acid. Since the particles were precipitated in acidic environment in the presence of excess of oxalic acid, it is not unusual that the ζ potential values were negative for all the samples. (Sengupta *et al.,* 2011). The negative charge as well as the magnitude of the potential is attributed to the presence of oxalate ions on the surface. Similar negative values of ζ potential was observed for copper oxalate (Vaidya *et al.,* 2008) and nickel oxalate particles synthesized in reverse micelles and for nickel oxalate particles prepared in the internal drops of water in oil emulsions (Sengupta *et al.,*2011).

Surface charges show an increase in ζ values when precipitates are formed in ethanolic oxalic acid. Particle precipitated in 10%, 25% and 50% ethanolic oxalic acid solutions resulted in ζ values of -24mV, -22.8 mV and -21.22 mV respectively indicating a decline of surface forces of attraction as well as repulsion. Greater electrostatic attraction between particles result in greater aggregation hence it is expected that the particles formed in ethanolic oxalic acid solutions will be less agglomerated than the particles formed in aqueous oxalic acid solutions. Morphology observed and particle size distribution also gives credence to these conclusions.

Field Emission Scanning Electron Microscopy

Figure 5.16 shows the FESEM images of copper oxalate particles precipitated at time intervals from 30 minutes to 4 hours. At 30 min precipitation time soft, flaky and plate like structures with well-defined boundaries are observed. Consolidation of the boundary regions of these particles is seen. A fairly wide size distribution of the particles can be made out from the SEM image. After 60 min precipitation time the particles appear to be more consolidated and more uniform in size. However, some large agglomerates are also seen. At 2 hr precipitation time the particles are not different from those observed after one hour and large agglomerates are not seen. After 180 min precipitation time particles are almost of uniform sizes ~170 nm. However, from the PSD (Figure 5.15) this size appears to be at the lowest end of the distribution.

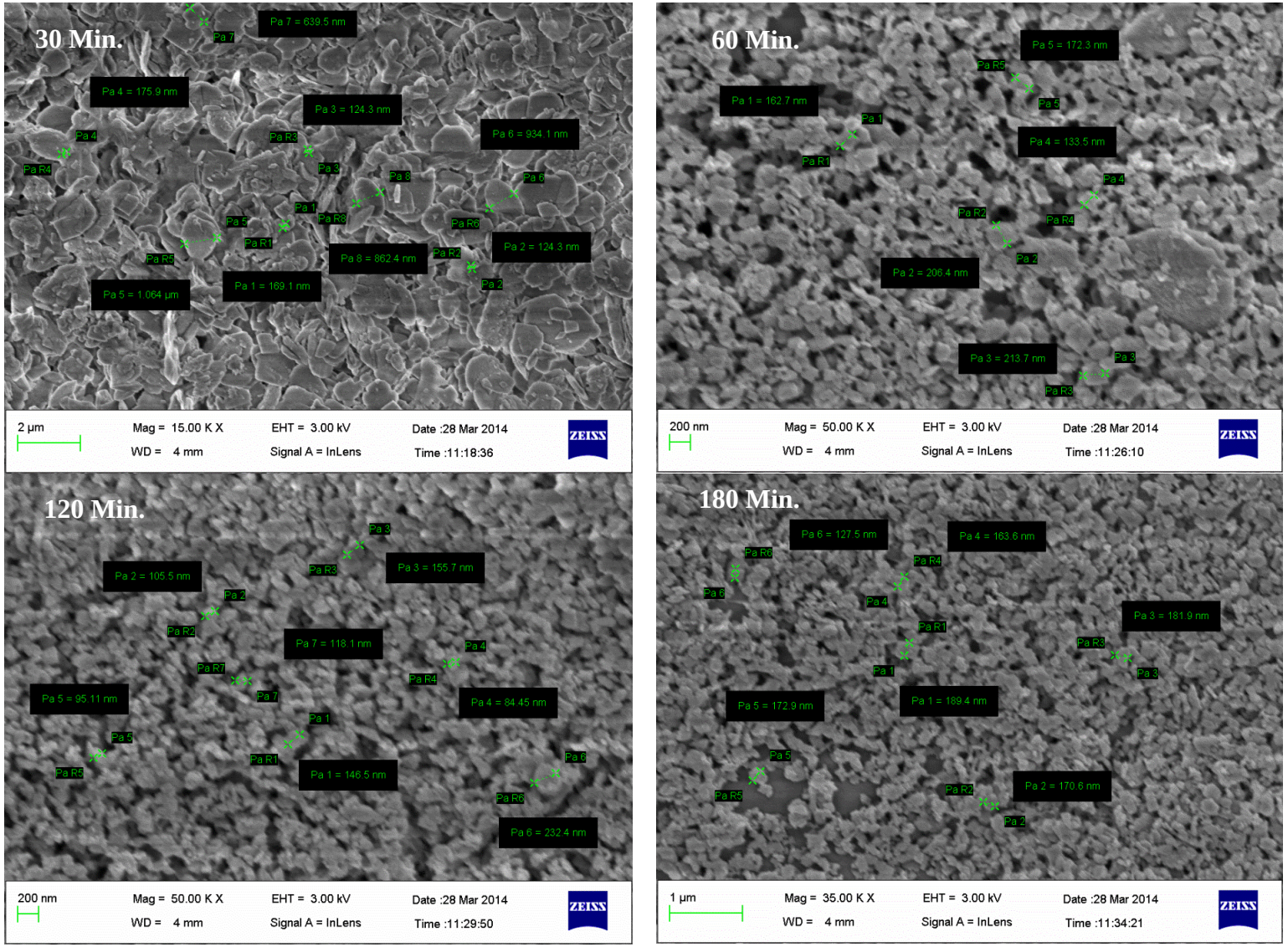

Fig. 5.16: FESEM of copper oxalate at varying PS times

Figure 5.17 a,b show FESEM images of copper oxalate particles E(10) and E(50) respectively. It is clearly seen from Figure 5.15 that most of the particles are smaller than 300 nm as the particle size distribution indicates. The particles are mostly well consolidated flat disks. Some large particles are seen in the background as well as some degree of aggregation is also observed. In Figure 5.17 b cluster of particles much smaller than 200 nm are observed. The overall view is of a porous aggregate sponge like structure, one can also make out that just too many particles are present in the frame, that is likely because in one single stage the oil phase was completely stripped.

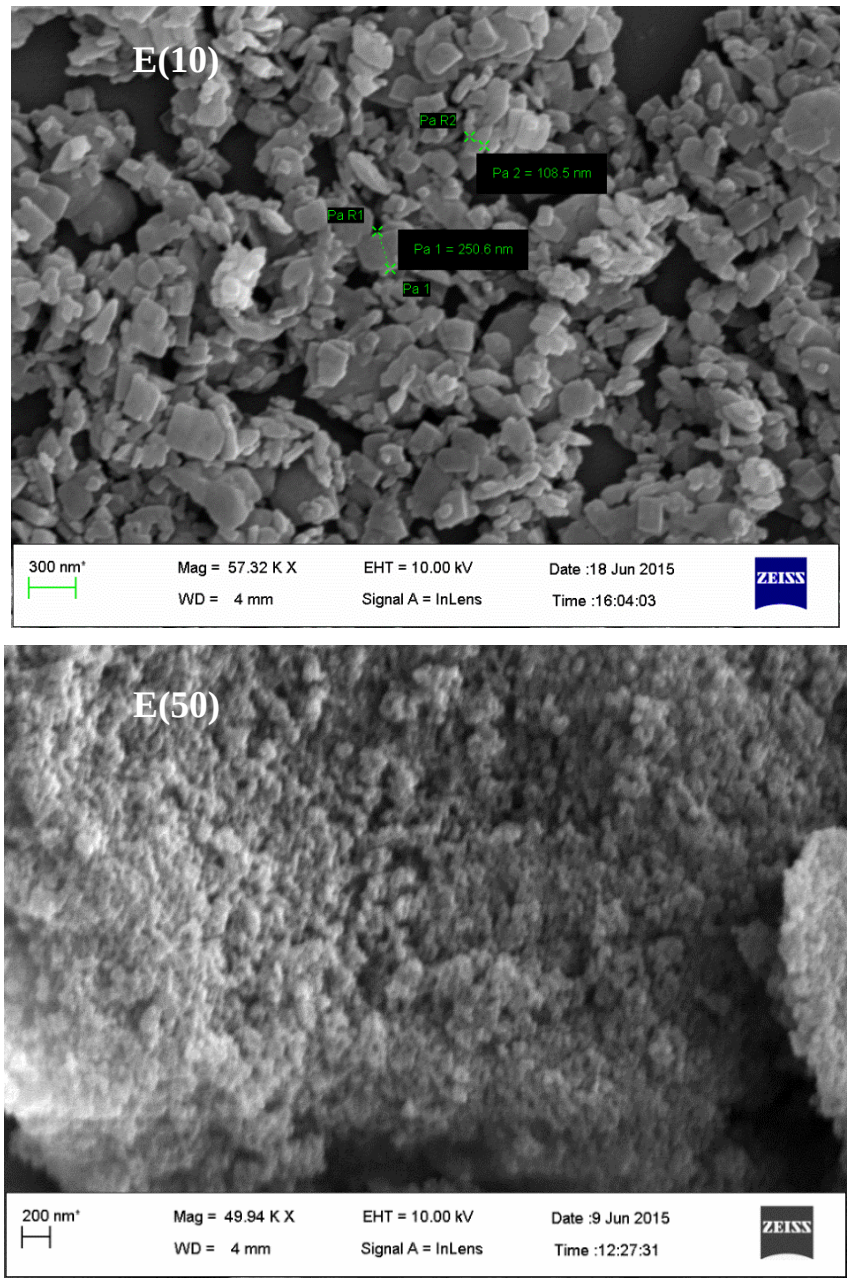

Fig. 5.17: FESEM of copper oxalate

Thermogravimetric Analysis

Copper oxalate is different than the other oxalates since water plays a minimal role in the structure and composition of copper oxalate in comparison to other oxalates which utilize oxygen from interlayer water molecules to complete co-ordination sphere (Dubernat and Pezerat, 1974). TGA of copper oxalate particles obtained for precipitation in oxalic acid solutions and 50% ethanolic oxalic acid solutions were recorded in an air atmosphere. Decomposition of copper oxalate in air atmosphere is given by

$$CuC_2O_4.H_2O \rightarrow CuC_2O_4 + H_2O \uparrow \quad (5.9)$$

$$CuC_2O_4 \rightarrow Cu_2O + 3CO_2 \uparrow + CO \uparrow \quad (5.10)$$

$$Cu_2O + CuC_2O_4 \rightarrow 3CuO + 2CO \uparrow \quad (5.11)$$

TGA plot for the oxalate sample precipitated in aqueous oxalic acid showed a loss due to decomposition of 55.65% which was much higher than the reported values of 47.57% for decomposition of the oxalate. On investigation it was inferred that during the process of precipitation-stripping the particles are precipitated at the oil-water interface and there is a possibility of oil phase getting entrapped between the particles. Such entrapped oil may not be completely removed by washing with water and keeps adhering to the particles, which resulted in high weight loss during decomposition. To validate this hypothesis an ethanol wash was given to the particles to wash out the adhering oil on particle surface, and after

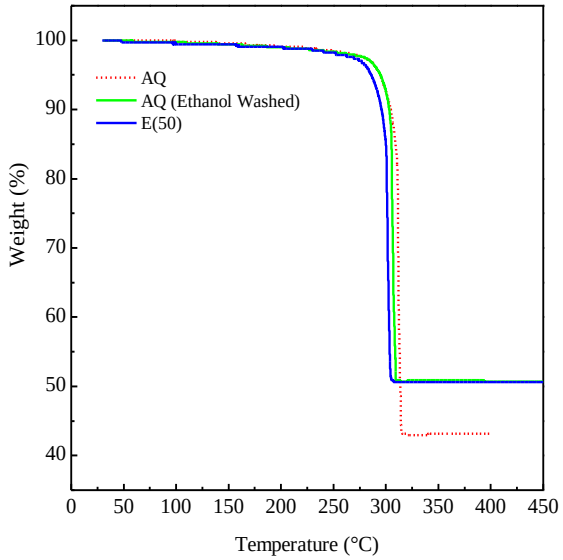

Fig. 5.18: TGA of copper oxalate

drying the particles, again a thermogram was run.

The thermograms generated for both these conditions, one for the water washed sample and other with ethanol washing are shown in Figure 5.18 which validates the inference of adhering oil phase. For the ethanol washed particles the weight loss of 1.02% before 225^{0}C is attributed to the emission of surface water. The weight loss of 48% from 225 ^{0}C to 312 ^{0}C is due to the decomposition of the oxalate closely matches with the theoretical value of 47.4% reported in the literature (Aimable *et al.*, 2011). The thermogram obtained for oxalates precipitated in 50% ethanolic oxalic acid sample E (50) was almost identical to that obtained with the ethanol washed sample and shows a weight loss of 0.89 % before 225^0 C and 47.91% from 225 ^{0}C to 312 ^{0}C.

5.8.2 Characterization of copper oxide particles

X-Ray Diffraction

Copper oxide was prepared by calcination of copper oxalate at 350 ^{0}C for three hours. The XRD analysis of the oxide formed revealed the presence of Cu_2O indicating that the decomposition of copper oxalate to oxide was not complete (Figure 5.19).

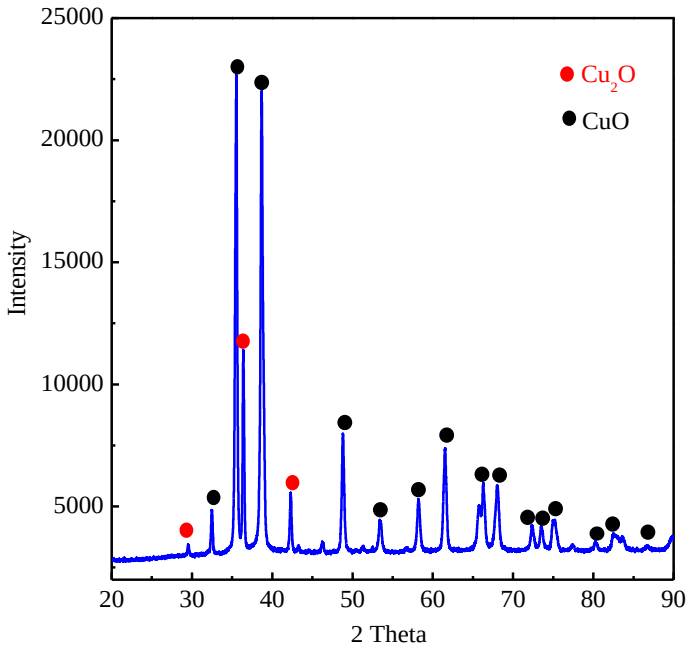

Fig. 5.19: XRD of copper oxalate calcined at 350^{0}C

Cu_2O is an intermediate product formed during the decomposition of oxalate to oxide. Donkova and Mehandjiev, (2005) reported that a temperature of 300^{0}C is insufficient for complete oxidation of Cu_2O to CuO and the conversion can be achieved at 400^{0}C (Christensen *et al.*,2014). Hence, the calcination temperature was increased to 400 ^{0}C while

retaining the same soaking time span to obtain complete decomposition of the oxalate to CuO.

The XRD patterns of the CuO calcined at 400^0C for samples AQ and E(50) are shown in Figure 5.20. The diffraction peaks for the oxides in both these cases could be indexed to the (110), (-111), (020), (-202), (220), (310) and (-113) reflections of monoclinic CuO phase (JCPDS No.5-661). No oxalate impurities were found in the sample indicating a high purity product obtained and complete decomposition of the oxalate to oxide. The average crystallite size of CuO as calculated from the Debye Sherrer equation for sample AQ is 26 nm and that for E(50) was 20 nm. The crystallite size for the oxide particles are $\pm$ 20% of the oxalates.

The lattice constants are found to be a = 4.65 Å, b = 3.41 Å and c = 5.11 Å, which are all in good agreement with the standard JCPDS data for monoclinic structured CuO for the particles precipitated in 50% ethanolic oxalic acid solution.

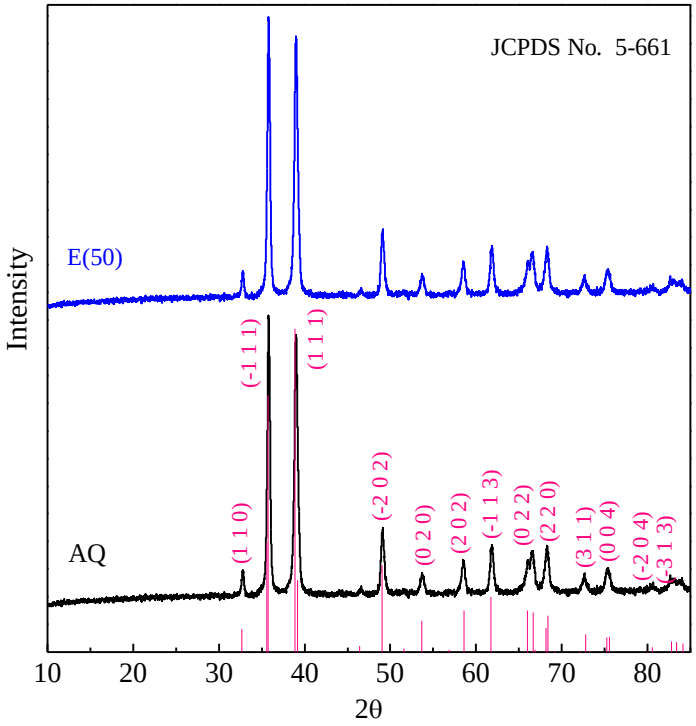

Fig. 5.20: XRD of copper oxide

Energy-dispersive X-ray spectroscopy

The EDX analysis (Figure 5.21) of copper confirmed pure CuO phase with Cu and O in stoichiometric proportions. The weight compositions for copper (Cu) and oxygen (O) were 80.58% and 19.42%, respectively and no other metals were detected. The chemical analysis of CuO also confirmed absence of any impurity indicating formation of pure copper oxide.

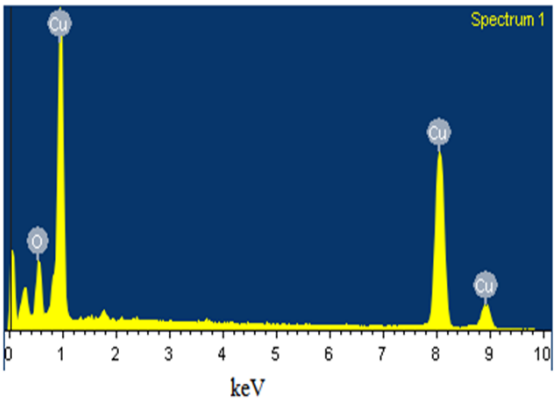

Fig. 5.21: EDX of copper oxide

Fourier transform infrared spectroscopy

The IR spectra (Figure 5.21) for sample AQ for copper oxide showed a broad band at 3420.11 cm^{-1} indicating the presence of surface hydroxyl groups and peaks observed at 530.64 cm^{-1} and 482 cm^{-1} are assigned to Cu-O bonds. Broad band at ~1642cm^{-1} corresponds to OH bending vibrations combined with copper atom.

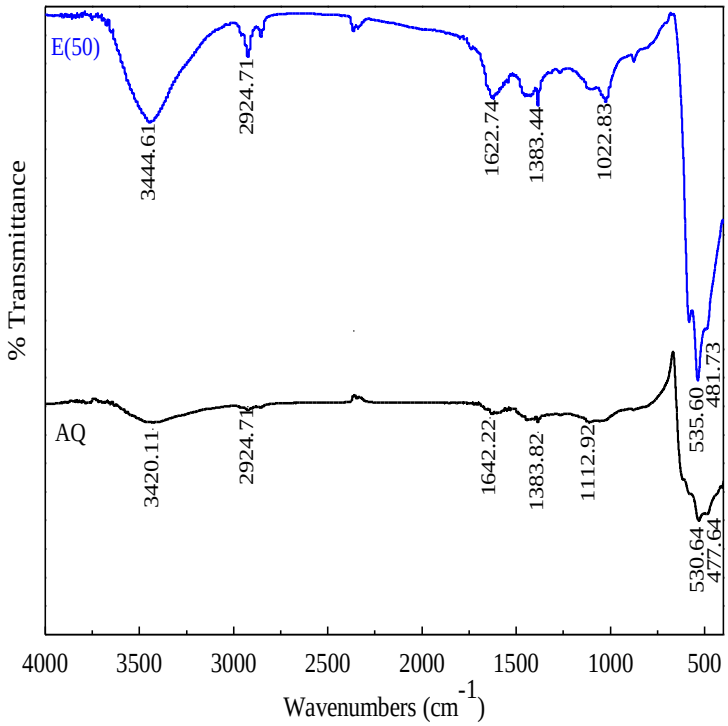

Fig. 5.22: FTIR spectra copper oxide

Band at ~1112 cm^{-1} is attributed to the OH bending vibrations of Cu-OH, band at 1383 cm^{-1} is due to CuO stretching, While the band at 2924 cm^{-1} is due to the asymmetrical CH_3 groups adsorbed on the surface of oxide particles. Similar bands were also observed in the spectra of sample E(50).

Field Emission Scanning Electron Microscopy

Morphology of copper oxide was investigated using FESEM. Figure 5.23 shows the FESEM images of copper oxide obtained by precipitation stripping from aqueous oxalic acid solution(AQ) and from 50% ethanolic oxalic acid (E50). CuO prepared from copper oxalate precipitated in aqueous oxalic acid are agglomerated with narrow size distribution with average size of ~ 200μm. CuO particles obtained from copper oxalate prepared in 50% ethanolic oxalic acid are low aspect ratio cylinder like particles with particle diameters of ~ 20nm and length ~40nm, there is clustering as well as agglomeration observed yielding a porous structure. Similar CuO structures have been reported by Dubal *et al.* (2013) prepared by potentiodynamic deposition which could find wide application as supercapacitors.

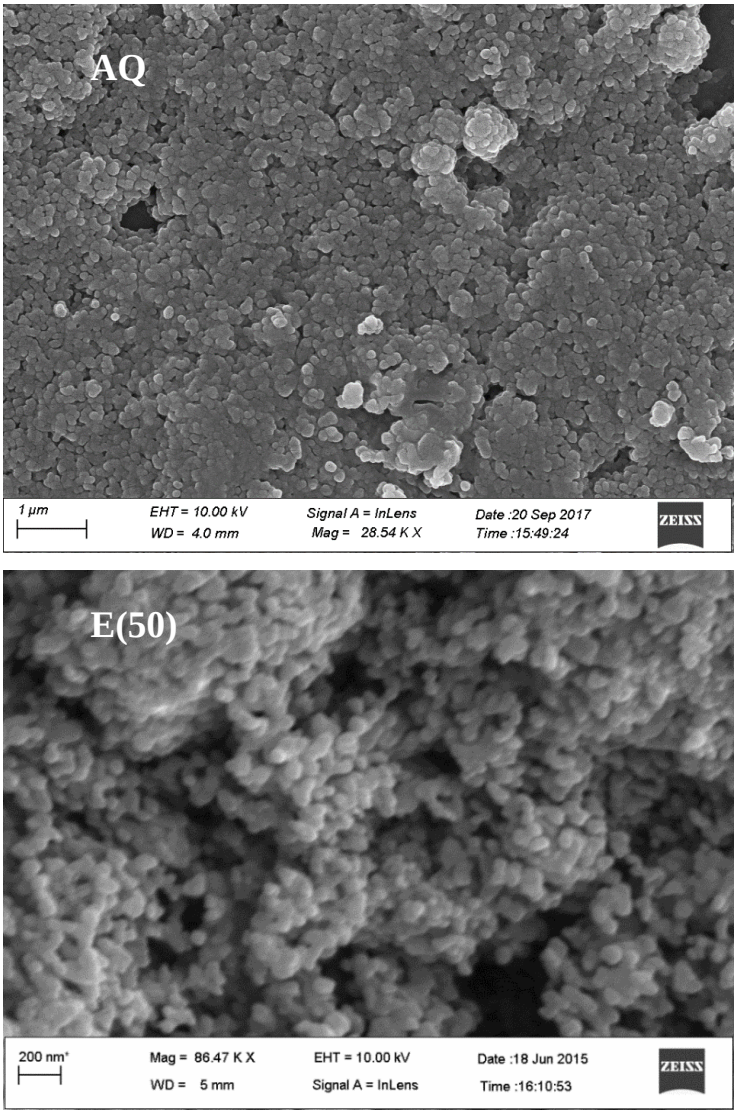

FIg. 5.23: FESEM of copper oxide

5.9 Process scheme for copper recovery

Post PS, the organic phase containing traces of copper was stripped using 1M sulfuric acid to recover copper prior to recycle of the organic phase. The organic phase was used up to five cycles with 0.2% decline in the extraction ability. Figure 5.24 shows the scheme for extraction/stripping and recovery of copper as copper oxide from the spent etchant. The etchant solution after copper recovery and ammonia make up can be recycled back for the etching operations and reused.

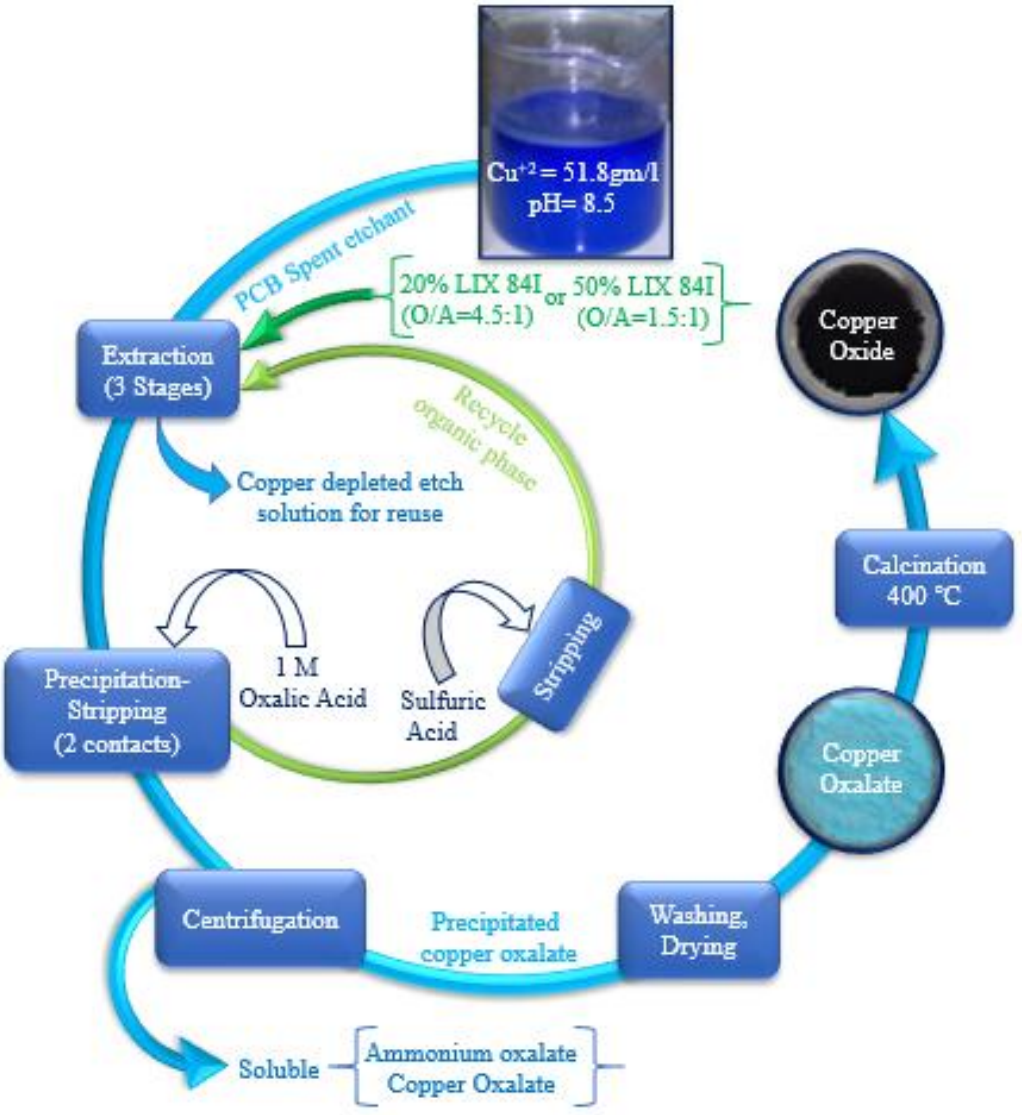

Fig. 5.24: Process scheme for copper recovery from spent PCB etch solutions

5.10 Application of copper oxide for reduction reaction of nitrobenzene to aniline

Aniline is an important aromatic amine used as a starting material for the manufacture of more than 300 chemical intermediates with diverse applications. Currently it is mainly used as a raw material in the production of methylene diphenyl diisocyanate (MDI), an intermediate in polyurethane manufacture accounting for over 95% of world aniline consumption in 2017. Global consumption of aniline is estimated at 7 million tons in 2016 likely to reach 9.3 million tons by 2022 at CARG of 4.9% per annum. The total consumption of aniline in India in 2016-17 was 86,000-tonnes. Production of aniline in India is done only at GNFC which was 41,450 tonnes during 2016-17. Thus more than 50% of India's requirement of aniline is met through imports.

There are several methods of synthesizing aniline using a variety of starting materials but nitrobenzene is the classical and the most frequently used feedstock. Around 85% of aniline is obtained by catalytic hydrogenation of nitrobenzene either in liquid or gas phase using supported metal catalysts and organic solvents. (Keypour *et al.*,2015). The reduction reaction of nitrobenzene to aniline has been used as a standard reaction to test the efficacy of catalysts and techniques developed by various investigators. Table 5.7 is a summary of investigations on synthesis of aniline from nitrobenzene.

Table 5.7: Synthesis of aniline from nitrobenzene

Condition	Catalyst	Parameters	Reference
Vapor phase hydrogenation	Metal supported on HAP catalyst in Fixed-bed tubular reactor	T=225-350^{0}C, P=1atm C=98%,S=99	Sudhakar *et.al.*, 2014
Homogeneous reduction	Bisacetylacetonato)palladiumll) in pyridine Solvent: petroleum ether	T=Room temp, P=1 atm, Yield: 90%	Datta *et al*., 1978
Chemoselective reduction	Copper nanoparticles and ammonium formate in ethylene glycol	T=120^{0}C, t=8-12 hr, C=75-90%	Saha and Ranu, 2008
Bayer gas phase process	Fixed-bed of NiS activated using copper or chromium	T=573-748K, S=99%	Weissermel and Arpe, 2008
BASF hydrogenation	Copper - chromium, barium and zinc oxides on a SiO_2 support	T=270-290 °C, P=1-5 bar, S=99.5 %	Heaton and Michigan, 1975
Huntsman liquid phase hydrogenation	55 % (w)of nickel supported on Kieselguhr	T=70- 150 °C, P=20-40 bar, C=99.7 %	Elena, 2017
Liquid phase catalytic reduction	Pd- or Pt-based catalysts, or their mixture in PFR	T=50°C to 100°C, P=1 to 5 MPa , Y=99%	Josef and Miroslav 2011

R= Type of reactor, T= Temp, t== residence time, P= pressure, C= conversion, S= selectivity, Y= yield

5.10.1 Reduction of nitrobenzene to aniline:

.

Nitrobenzene was reduced to aniline using sodium borohydride as the reducing agent and copper oxide particles as the catalyst. Sodium borohydride is well known as a good reducing agent but in absence of a catalyst its reducing power is limited. However, sodium borohydride with transition metal salts results in enhanced potential to reduce various functional groups. (Yoo and Lee, 1990).

The reduction reaction was carried out using methanol as the solvent. Nitrobenzene (5 mmol) was dissolved in methanol and copper oxide particles were added and stirred for 5 minutes, $NaBH_4$ (15 mmol) was slowly added and stirred at the selected temperature for a specified period of time. Reaction was monitored using TLC. On completion, the reaction mixture was filtered and solvent methanol was evaporated under vacuum. The crude residue was then partitioned between brine and methylene chloride and the combined organic layers were dried over anhydrous Na_2SO_4 which was filtered off and the solvent was removed under vacuum to yield aniline. The reusability and the recyclability of the catalyst were also investigated.

The reduction reaction of nitrobenzene to aniline in the presence of sodium borohydride can be represented by Equation 5.10

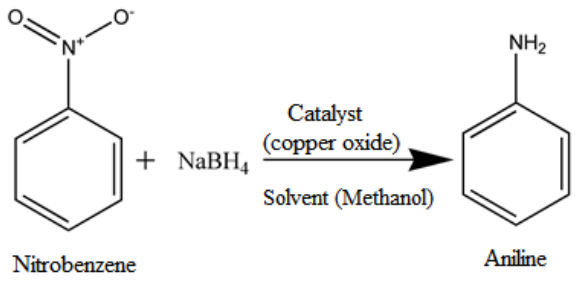

(5.10)

Preliminary reactions were carried out at 60^0C with a molar ratio of nitrobenzene to $NaBH_4$ ratio (N/S) of 1:3 for 3 hr reaction time in the absence of catalyst. It was found that in the absence of catalyst the reaction was ineffective. Increasing the reaction time, also resulted in no enhancement of nitrobenzene conversion.

The effect of parametric variations on the reduction of nitrobenzene to aniline was investigated at different temperatures, catalyst concentrations and reaction time spans. The copper oxide catalyst used for the reduction reaction was prepared by the calcinations of

copper oxalate sample (AQ). The optimal time required for the conversion of nitrobenzene to aniline was determined by varying the reaction time from 1 hr to 3 hrs using 10 mol% catalyst at a temperature of 60^0C. Increasing the reaction time from 1 hr to 3hrs resulted in an increase in the conversion of nitrobenzene from 19.1% to 99.9% (Figure 5.25a).

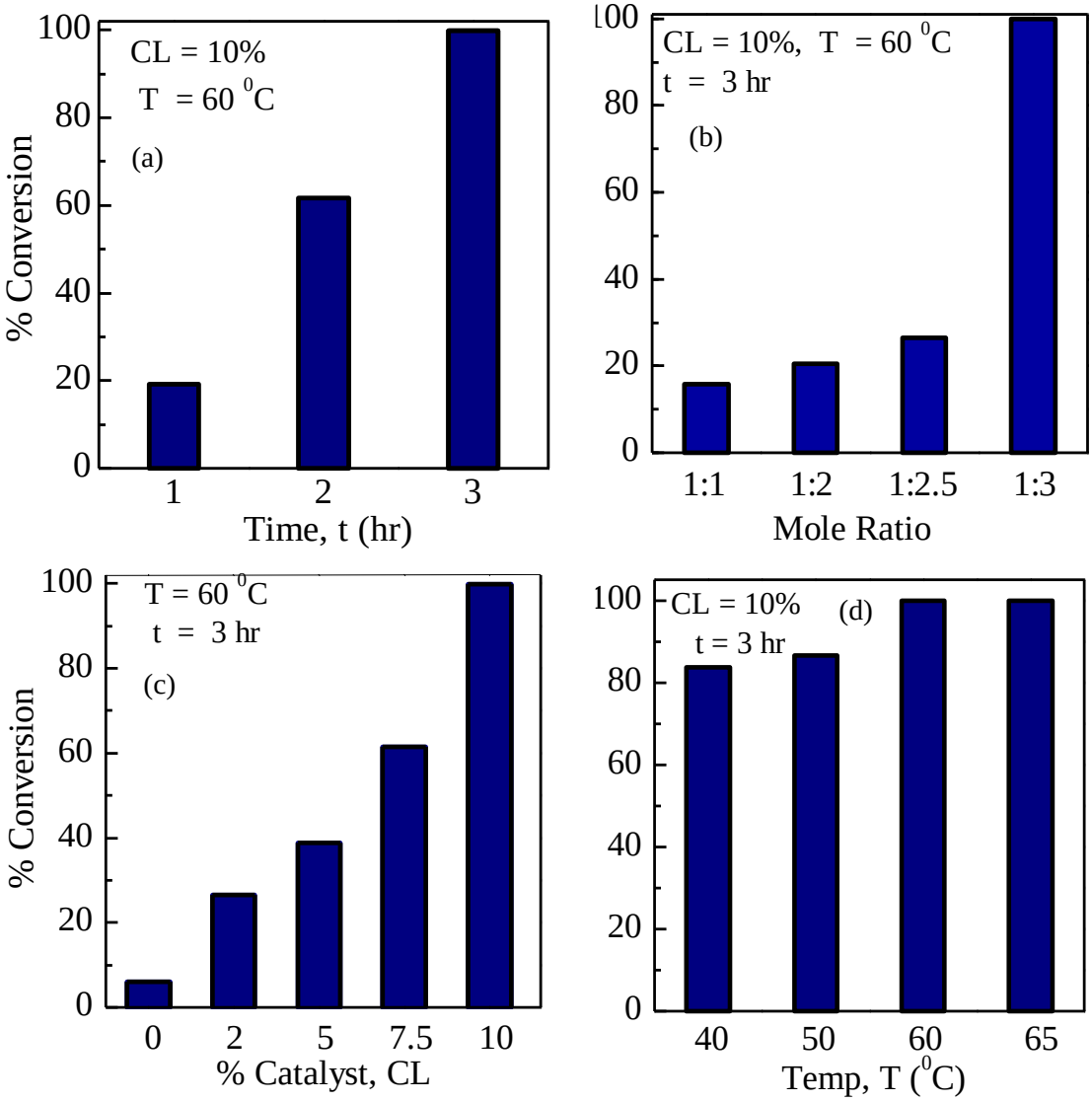

Fig. 5.25:Effect of parametric variations on percentage conversion

There was hardly any significant increase in conversion when N/S ratio was increased from 1:1 to 1:2.5. However, further increase in the ratio to 1:3 resulted in a substantial increase in the conversions (Figure 5.25b). Increase in catalyst concentration from 2 to 10 mol% at the reaction conditions of 60 °C, N/S mole ratio of 3 and reaction time of 3 hr results in the increase of nitrobenzene conversion from 26.5% to 99.9% (Figure 5.25c). Further increase in the catalyst concentration did not increase the conversion. Increasing the temperature from

40 to 60 °C using 10 mol % catalyst, the conversion increased from 83.3% to 99.9% (Figure 5.25d).

The recycle capability of CuO was investigated by conducting the reduction reactions at the optimized conditions of 10 mole % catalyst loading, 60 °C temperature, 3 hr reaction time, with N/S mole ratio of 1:3. The catalyst particles were washed and dried each time after use. The catalyst particles could be reused for 4 cycles without any significant decline in activity and drop in the conversion (Figure 5.26).

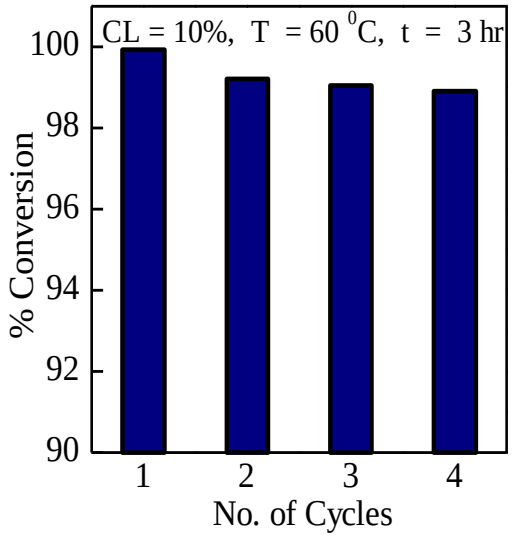

Fig. 5.26: Reusability of catalyst

Reactions were also carried out at the optimized conditions with CuO particles prepared by PS copper oxalate in 50% ethanolic oxalic acid and CuO procured from Sigma Aldrich (50 nm size). It was found that the CuO particles obtained from both these sources also exhibited the same potential to catalyze the reduction reaction. The surface area of the particles as determined by BET analysis was 2 m^2/g. Particles prepared by precipitation in 50% ethanolic oxalic acid had a surface area of 1.79 m^2/g.

Figure 5.27 shows the plausible reaction mechanism for reduction of nitrobenzene to aniline. In the first step, in the presence of copper oxide and sodium borohydride the single nitrogen-oxygen bond is hydrogenolysed, and an oxygen atom lost, to produce the first intermediate. In second stage the addition of two hydrogen atoms across the remaining nitrogen-oxygen double bond to give the compound, phenyl hydroxylamine. In the last, third step phenyl hydroxylamine loss second oxygen to form aniline as the final product.

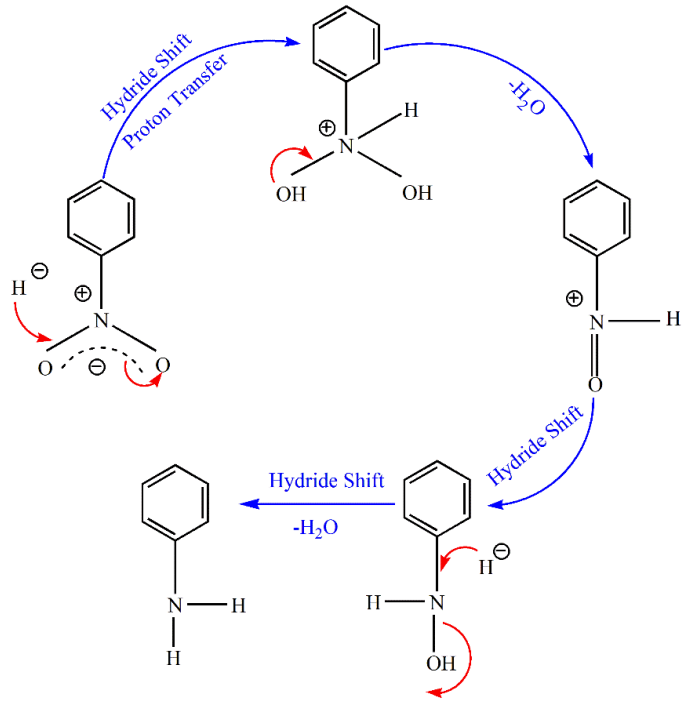

Fig. 5.27: Reaction mechanism

5.11 Conclusions

There are around 200 PCB manufacturers in India of which more than 60 per cent are very small and in the unorganized sector. Ammoniacal etchants, ammonium chloride or ammonium sulfate are the most widely used etchants in the PCB industry. Spent etching solutions obtained from the PCB industry contain a large amount of copper which can be recovered and recycled for further reuse. Almost one billion cubic meter of waste etchant is being generated annually from the PCB industry worldwide accounting for more than 70,000 tons of copper being lost if unclaimed. A spent ammoniacal etching solution collected from a PCB manufacturing industry in Vadodara containing 50 g/L copper having an initial pH value of 8.5 was used to recover copper. An extraction-stripping scheme was developed using LIX 84 I as the extractant in kerosene solvent and the PS technique for regenerating the extractant and simultaneously producing copper oxalate particles. The copper oxalate thus obtained was calcined to obtain copper oxide that has considerable commercial potential.

Effect of pH on copper extraction was investigated and a maximum extraction was obtained at a pH value of 8.9. Increase in extractant concentration from 10% (v/v) to 50% (v/v) was a monotonically increasing function. Extraction using 20% (v/v) and 50% (v/v) were

investigated at organic to aqueous ratios of 4.5:1 and 1.5:1 respectively. In both the cases three equilibrium stages as indicated by McCabe-Thiele plots. Stripping of the fully loaded organic phase with 50% extractant using 1M oxalic acid was achieved in two contacts with use of fresh acid at each time.

Stripping of the loaded organic phase was also performed using ethanolic oxalic acid solutions. With 1 M oxalic acid in 10% ethanolic oxalic acid solutions two stages were required for complete stripping, while with 25% and 50% ethanolic-oxalic acid solutions stripping was achieved in a single stage. The stripping was complete in all cases in one-hour contact between oil phase and oxalic acid. With 50% ethanolic solutions a milky white dispersion resulted on agitation of the oil and water phase that took some time to separate. The particles produced in aqueous oxalic acid were of wide size distribution and quite aggregated while particles formed in 50% ethanolic oxalic acid were very small in size in the range of below 50 nm.

Particles were characterized by XRD, FTIR, FESEM etc. and were identified as pure copper oxalate matching with necessary JCPDS standard. TGA of particles identified decomposition patterns and oxalate particles were calcined to get copper oxide by soaking at 400^0 C for 3 hours in a tube furnace. The oxide particles were also characterized by XRD, EDX, FTIR, the morphology was observed by FESEM, particle size distribution was determined and surface charge (zeta potential) were measured. Pure CuO particles were obtained matching JCPDS standards, no other impurities were observed. Particles were aggregated and had surface charge of -34.29 mV for particles formed in oxalic acid solution and was -21.22mV for particles obtained in 50% ethanolic oxalic acid solutions for the other cases the zeta potential values were in between the above two values.

It is interesting to note that copper extraction from into hydroxyoximes from ammoniacal solutions is almost always accompanied with ammonia transfer. However, maximum loading of copper minimizes the transfer of ammonia in the organic phase. During the reclamation of copper by conventional stripping process during electrowinning a buildup of ammonium sulfate is observed after recycle of spent electrolyte over a period of time. While in precipitation stripping copper is reclaimed as copper oxalate and there is separation of the solid from the aqueous phase in which ammonium oxalate is soluble. Hence, precipitation

stripping offers an inherent advantage during the reclamation of copper avoiding ammonium sulfate precipitation.

The copper oxide prepared was used to catalyze the reduction of nitrobenzene to aniline and the effects of various parameters were investigated. The overall conversion was found to be over 98% with 100% selectivity. The catalyst could be recycled a number of times without any loss of activity.

Thus the copper present in spent PCB ammoniacal etch solutions was reclaimed by solvent extraction using LIX 84I followed by PS using oxalic acid to get copper oxalate particles, which were calcined to get pure CuO particles that have considerable commercial potential. This process can be adopted by small scale PCB manufacturers.

References

- Aimable A, Puentes AT, Bowen P. Synthesis of porous and nanostructured particles of CuO via a copper oxalate route. *Powder Technol.* 2011; 208(2): 467-471.
- Alguacil FJ, Alonso M. Recovery of copper from ammoniacal/ammonium sulfate medium by LIX 54. *J Chem Technol Biotechnol*. 1999; 74: 1171–1175.
- Allen DM, Almond HJA. Characterization of aqueous ferric chloride etchants used in industrial photochemical machining. *J Mater Process Technology*. 2004; 149: 238–245.
- Avery JM, Moleux PG. process waste minimization and treatment. In: *Printed Circuits Handbook*. 2007; 60.6. Coombs CF (ed.). McGraw-Hill Handbooks, New York.
- Batueva TD, Radushev AV, Gusev VY. Extraction of copper (II) from weakly acid and ammonia media with N',N'- dialkylhydrazides of aliphatic carboxylic acids. *Russ J Appl Chem*. 2009; 82: 1997–2001.
- C. A. Heaton, Y. 1975, Michigan: Ann Arbor Science of modern industrial chemist, Blackie: Glasgow. 1991; 392-393. Notion Press, Chennai.
- Cakir O. Copper etching with cupric chloride and regeneration of waste etchant. *J Mater Proces. Technol.* 2006; 175: 63-68.
- Cakir O. Copper etching with cupric chloride and regeneration of waste etchant. 2003; 139–142. In: *Proceedings of the 12th International Scientific Conference on Achievements, Mechanical and Materials Engineering* (AMME 2003), Gliwice, Poland.

- Cakir, O. Review of etchants for copper and its alloys in wet etching processes. *Key Engineering Materials* 2008; 364: 460-465.
- Chancerel P, Meskers CEM, Hageluken C, Rotter V. Assessment of precious metal flows during preprocessing of waste electrical and electronic equipment. *J Industrial Ecology*. 2009; 13: 791–810
- Chen G. Electrochemical technologies in wastewater treatment. *Sep Purif Technol.* 2004; 38(1): 11-41.
- Choubey PK, Panda R, Jha MK, Lee JC, Pathak DD. Recovery of copper and recycling of acid from the leach liquor of discarded printed circuit boards (PCBs). *Sep Purif Technol.* 2015; 156: 269–275.
- Coombs CF. *Printed Circuits Handbook.* 2007; 6^{rth}Edn. McGraw-Hill Handbooks, New York.
- Cyrille AD, Edith KK, Marius NP, Bernadette ABE, Henri AK. Experimental and theoretical studies of oxalic acid dissociation in water-ethanol solvents. *IJSR.* 2015; 4: 280-286.
- Datta MC, Saha CR, Sen D. Studies on the reduction of nitrobenzene to aniline catalyzed by bis(acetylacetonato)palladium(II)-pyridine system. *J Appl Chem Technol & Biotechnol.* 1978; 28(11): 709-711.
- De-liang LI, Ren-hua. Selective separation of copper by membrane- electro-winning and its application in etchant recycling. *J. Cent South Univ Technol*. 2005; 12: 10–1
- Donkova B, Mehandjiev D. Review thermal-magnetic investigation of the decomposition of copper oxalate-a precursor for catalysts. *J Mater Sci*. 2005; 40(15): 3881-3886.
- Duan H, Hou K, Li J, Zhu X. Examining the technology acceptance for dismantling of waste printed circuit boards in light of recycling and environmental concerns. *J Environ Manage*. 2011; 92: 392–399.
- Dubernat J, Pezerat H. Stacking faults in oxalates dihydrates of the divalent metals of the mangesian series (Mg, Fe, Co, Ni, Zn, Mn). *J Appl Cryst* 1974; 7: 387-393.
- Elena D. Milliken, Terry J. Detrie, George E. Sakoske. Copper oxide infrared pigment. 2017; In: *US Patent 20170015836 A1*.
- Fouad OA, Abdel Basir SM. Cementation-induced recovery of self-assembled ultrafine copper powders from spent etching solutions of printed circuit boards. *Powder Technol.* 2005; 159: 127–134.

- Frias B. In: *Source reduction technologies in california printed circuit*. Davis G, Rooney PM. (Eds.) California Environmental Protection Agency. 1999; (539): 1-30.
- Frias C, Raychaudhuri A, Palma J, Diaz G. Development of new-concept clean technologies to extract metals from primary and secondary sources. In: *Environmental & waste management*. Bandopadhyay A, Rakesh Kumar, Ramachandrarao P. (eds.) 2002; 165-173.
- Fries B. Source reduction technologies in California printed circuit board manufacture. 1999; 539: 1-30. Davis G, Rooney PM (eds.), California Environmental Protection Agency.
- Ghosh B, Ghosh M, Parhi P, Mukherjee P, Mishra B. Waste printed circuit boardsrecycling: an extensive assessment of current status. *J Clean Prod* 2015; 94: 5-19.
- Giannopoulou DI, Panias LD, Paspaliaris PI. Copper recovery from spent ammoniacal etching solutions. 2003; 3: 1035-1046. In: *Proceedings of EMC.*
- Gu, Y, Wu Y, Xu M, Wang H, Zuo T. The stability and profitability of the informal WEEE collector in developing countries A case study of China. *Resour Conserv Recycl.* 2016; 107: 18–26.
- Gurian MI , Etching process and technology. In: *Printed Circuits Handbook.* 2007; 34.1-34.30. Coombs CF (ed.). McGraw-Hill Handbooks, New York.
- Hadi P, Xu M, Lin CSK, Hui CW, McKay G. Waste printed circuit board recycling techniques and product utilization. *J Hazard Mater*. 2015; 283: 234–243.
- Hall WJ and Williams PT. Processing waste printed circuit boards for material recovery. *Circuit World*. 2007; 33: 43–50.
- He J, Duan C. Recovery of metallic concentrations from waste printed circuit boards via reverse floatation. *Waste Manag.* 2017; 60: 618-628.
- He W, Li G, Ma X, Wang H, Huang J, Xu M, Huang, C. WEEE recovery strategies and the WEEE treatment status in China. Journal of Hazardous Materials. 2006; 136: 502-512
- Hu J, Chen Q, Hu H, Chen X, Ma Q, Yin Z. Extraction behavior and mechanism of Cu (II) in ammoniacal sulfate solution with β-diketone. *Hydrometallurgy.* 2012: 127–128: 54–61.
- Hu J, Chen Q, Hu H, Jiang Z, Wang D, Wang S, Li Y. Microscopic insights into extraction mechanism of Copper (II) in ammoniacal solutions studied by X-ray

absorption spectroscopy and density functional theory calculation. *J Phys Chem A.* 2013; 117: 12280–12287.

- Huang Z, Xie F, Ma Y. Ultrasonic recovery of copper and iron through the simultaneous utilization of Printed circuit boards (PCB) spent acid etching solution and PCB waste sludge. *J Hazard Mater.* 2011; 185: 155–161.
- Isildar A, Rene ER, Hullebusch ED, Lens PNL. Two-Step leaching of valuable metals from discarded printed circuit boards, and process optimization using response surface methodology. *Adv Recycl Waste Manag*. 2017; 2(2): 1-9.
- Isildar. Biotechnology for metal recovery from electronic waste and printed circuit boards. In: *Waste Electrical and Electronic Equipment Recycling: Aqueous Recovery Methods.* 2018; 241-269. Veglio F, Birloaga I. (eds.) Woodhead Publishing, Elsevier, United Kingdom.
- Jongen N, Bowen P, Lemaitre J, Valmalette J, Hofmann H. Precipitation of self-organized copper oxalate polycrystalline particles in the presence of hydroxypropylmethylcellulose (HPMC): Control of Morphology. *J Colloid Interface Sci.* 2000; 226: 189–198.
- Josef P, Miroslav P. A method for the catalytic reduction of nitrobenzene to aniline in the liquid phase. In: *European Patent Application EP 2471768 A1*, 2011.
- Keskitalo T, Tanskanen J, Kuokkanen T. Analysis of key patents of the regeneration of acidic cupric chloride etchant waste and tin stripping waste. *Resour Conserv Recycl.* 2007; 49: 217–243.
- Keypour H, Noroozi M, Rashidi A, Shariati Rad M. Application of response surface methodology for catalytic hydrogenation of nitrobenzene to aniline using ruthenium supported fullerene nanocatalyst. *Iran J Chem Chem Eng.* 2015; 34(1): 21-32.
- Khandpur RS. Printed Circuit Boards: Design, Fabrication, Assembly and Testing. 2005. 365-382. Tata McGraw-Hill Education Pvt. Ltd.
- Kim J, Jeong S, Cho Y, Kim K. Eco-friendly manufacturing strategies for simultaneous consideration between productivity and environmental performances: A case study on a printed circuit board manufacturing. *J Clean Prod.* 2014; 67: 249–257.
- Kumari A, Kumar M, Lee J, Prasad R. Clean process for recovery of metals and recycling of acid from the leach liquor of PCBs. *J Clean Prod.* 2016; 112: 4826-4834
- Kyuchoukov G, Bogacki MB, Szymanowski J. Copper extraction from ammoniacal solutions with LIX 84 and LIX 54. *Ind Eng Chem Res*. 1998; 37: 4084–4089.
- LaDou J. Printed circuit board industry, *Int J Hyg Environ Health*. 2006; 209: 211–219.

- Lee CJ and Chan CC. Extraction of ammonia from a dilute aqueous solution by emulsion liquid membrane: Experimental studies in batch system. *Ind Eng Chem Res.*1990; 29: 96-100.
- Lee MS, Ahn JG, Ahn JW. Recovery of copper, tin and lead from the spent nitric etching solutions of printed circuit board and regeneration of the etching solution. *Hydrometallurgy*. 2003; 70: 23–29.
- Li N, Lu X, Zhang S. A novel reuses method for waste printed circuit boards as catalyst for wastewater bearing pyridine degradation. *Che Eng J.* 2014; 257: 253–261.
- Liang QW, Hu HP, Fu W, Ye T, Chen QY. Recovery of copper from simulated ammoniacal spent etchant using sterically hindered beta-diketone. *Trans Nonferrous Met Soc.* 2011; 21: 1840-1846.,
- Lide DR. CRC Handbook of Chemistry and Physics, 84th ed, 2004; 127-129. CRC Press LLC.
- Liu S, Hou H, Liu X, Duan J, Yao Y, Liao Q, Li J, Yang Y. Recycled hierarchical tripod-like CuCl from Cu-PCB waste etchant for lithium ion battery anode. *J Hazard Mater.* 2017; 324: 357–364.
- Lurdes M, Gameiro F, Machado RM, Rosinda M, Ismael C, Teresa M, Carvalho JMR. Copper extraction from ammoniacal medium in a pulsed sieve-plate column with LIX 84-I. *J Hazard Mater*. 2010; 183: 165–175.
- Martell AE, Smith RM. Critical Stability Constants of Metal Ion Complexes, Part B, Organic Ligands. 1977. *Pergamon Press*.
- Meng L, Zhong Y, Wang Z, Chen K, Qiu X, Cheng H, Guo Z. Supergravity separation for Cu recovery and precious metal concentration from waste printed circuit boards. *ACS Sustain Chem. Eng.* 2018; 6: 186–192.
- Nakahara H. Types of printed wiring boards. In: *Printed Circuits Handbook*. 6th Ed. 2007; 115-128. Coombs CF (ed.). McGraw-Hill Handbooks, New York.
- Nathsarma KC, BhaskaraSarma PVR. Processing of ammoniacal solutions containing copper, nickel and cobalt for metal separation. *Hydrometallurgy.*1993; 33: 197–210.
- Ochromowicz K, Jeziorek M, Wejman K. Copper (II) extraction from ammonia leach solution. *PhysicochemProbl Miner Process*. 2014; 50: 327–335.
- Panias D, Giannopoulou I, Paspaliaris I. Copper electrowinnining from the ammoniacal etching effluents of printed circuit boards industry. 2002; 1137-1142. In: *Proceedings SWEMP 2002*, Ciccu R.(ed.), Cagliari, Italy.

- Rahimi-Nasrabadi M, Pourmortazavi SM, Davoudi-Dehaghani AA, Hajimirsadeghi SS, Zahedi MM. Synthesis and characterization of copper oxalate and copper oxide nanoparticles by statistically optimized controlled precipitation and calcination of precursor. *Cryst Eng Comm*. 2013; 15: 4077.
- Clark RH. Handbook of Printed Circuit Manufacturing. 2012. Springer Science & Business Media.
- Rice NM, Nedved M, Ritcey GM. The extraction of nickel from ammoniacal media and its separation from copper, cobalt and zinc using hydroxyoxime extractants I. SME-529. *Hydrometallurgy*. 1978; 3(1): 35-54.
- Rosinda M, Ismael C, Jorge M, Carvalho R. Copper recovery from spent ammoniacal etching solutions. 2002; 781–786. In: *Proceedings of International Solvent Extraction Conference* (ISEC'2002); Sole KC, Cole PM, Preston JS, Robison DJ. (ed.), Chris van Rensburg Publications Ltd., SouthAfrica.
- Rosinda M, Ismael C, Lurdes M, Gameiro F, Carvalho JMR. Extraction equilibrium of copper from ammoniacal media with LIX 54. *Sep Sci Technol.* 2004; 39: 3859–3877.
- Saha A, Ranu B. Highly chemoselective reduction of aromatic nitro compounds by copper nanoparticles/ammonium formate. *J Org Chem* 2008; 73: 6867–6870.
- Schuerink GA, Slomp M, Wits WW, Legtenberg R, Kappel EA. Modeling printed circuit board curvature in relation to manufacturing process steps. *Proc CIRP*. 2013; 9: 55–60.
- Sengupta B, Bhakhar MS, Sengupta R. Extraction of copper from ammoniacal solutions into emulsion liquid membranes using LIX 84-I. *Hydrometallurgy*. 2007; 89 (3−4): 311−318.
- Sengupta B, Bhakhar MS, Sengupta R. Extraction of zinc and copper-zinc mixtures from ammoniacal solutions into emulsion liquid membranes using LIX 84-I Hydrometallurgy. 2009; 99(1-2): 25-32.
- Sengupta B, Tamboli CA, Sengupta R. Synthesis of nickel oxalate particles in theconfined internal droplets of w/o emulsions and in systems without space con-finement. *Chem Eng J.* 2011; 169: 379–389.
- Shah K, Gupta K, Sengupta B. Selective separation of copper and zinc from spent chloride brass pickle liquors using solvent extraction and metal recovery by precipitation-stripping. *J. Environ. Chem. Eng.* 2017; 5: 5260–5269.
- Shokri A, Pahlevani F, Levick K, Cole I, Sahajwalla V. Synthesis of copper-tin nanoparticles from old computer printed circuit boards. *J. Clean Prod*. 2017; 142: 2586–2592.

- Stone FE. Electroless copper in printed wiring board fabrication. In: *Electroless Plating: Fundamentals and Applications.* 1990; 331-375. Mallory G, Hajdu J (eds.), AESF, New York.
- Stuhlpfarrer P, Luidold S, Antrekowitsch H. Recycling of waste printed circuit boards with simultaneous enrichment of special metals by using alkaline melts: A green and strategically advantageous solution. *J Hazard Mater*. 2015; 30: 17−25.
- Sze YKP, Wong JC. A study of a solvent extraction method for the regeneration of ammonical etching solutions of copper. *Environ Technol*. 2008; 15(8): 37–41.
- Thakur P, Joshi SS. Effect of alcohol and alcohol/water mixtures on crystalline structure of CdS nanoparticles. *J Exp Nanosci*. 2012; 7(5): 547-558.
- Vaidya S, Rastogi P, Agarwal S, Gupta SK, Ahmad T, Antonelli AM, Ramanujachary KV, Lofland SE, GangulI AK. Nanospheres, nanocubes, and nanorods of nickel oxalate: Control of shape and size by surfactant and solvent. *J Phys Chem C*. 2008; 112(33): 12610-12615.
- Wang H, Zhang S, Li B, Pan D, Wu Y, Zuo T. Recovery of waste printed circuit boards through pyrometallurgical processing: A review. *Resour Conser Recycl*. 2017; 126: 209–218.
- Wang S, Li J, Narita H, Tanaka M. Equilibrium modeling of the extraction of copper and ammonia from alkaline media with the extractant LIX84I. 2017; 58: 1427-1433. In: *Mater Trans.*
- Wang S, Li J, Narita H, Tanaka M. Modeling of equilibria for the solvent extraction of ammonia with LIX84-I. *Solvent Extr Res Dev.* 2017; 24: 71–76.
- Wang ZL, Liu Y, Zhang Z (eds.) 2003; Handbook of Nanophase and Nanostructured Materials. Springer.
- Weissermel K, Arpe H. Industrial Organic Chemistry, 1997; 3rd Edn. VCH Publishers Inc. John Wiley & Sons, New York, USA.
- Wieszczycka K, Kaczerewska M, Krupa M, Parus A, Olszanowski A. Solvent extraction of copper (II) from ammonium chloride and hydrochloric acid solutions with hydrophobic pyridineketoximes. *Sep Purif Technol.* 2012; 95: 157–164.
- Winnubst L, de Veen PJ, Ran S, Blank DHA. Synthesis and characteristics of nanocrystalline 3Y-TZP and CuO powders for ceramic composites. *Ceram Int.* 2010; 36(3): 847-853.

- Wyman J. The dielectric constant of mixtures of ethyl alcohol and water from -5 to 40 ^{0}C. *J Am Chem Soc*. 1931; 53 (9): 3292–3301.
- Xiu Z, Li J, Li X, Huo D, Sun X, Ikegami T, Ishigaki T. Nanocrystalline Scandia Powders Via Oxalate Precipitation: The Effects of Solvent and Solution pH. *J Am Ceram Soc*. 2008; 91: 603-606.
- Xu Y, Li J, Liu L. Current Status and Future Perspective of Recycling Copper by Hydrometallurgy from Waste Printed Circuit Boards. *Procedia Environ Sci.* 2016; 31: 162-170.
- Yang M, He J, Hu X, Yan C, Cheng Z. Synthesis of nanostructured copper oxide via oxalate precursors and their sensing properties for hydrogen cyanide gas. *Analyst*. 2013; 138: 1758-1763.
- Yang Z, Huang C, Ji X, Wang Y. A new electrolytic method for on-site regeneration of acidic copper (II) chloride etchant in printed circuit board production. *Int J Electrochem Sci*. 2013; 8: 6258–6268.
- Yaro AS, Hanna ZN. Copper Recovery from spent etchant cupric chloride solution by electrowinning method. *J of Engineering* 2007; 13: 1344–1353.
- Yoo SE, Lee SH. Reduction of organic compounds with sodium borohydride-copper (II) sulfate system. *Synlett*. 1990; 7: 419-420.
- Yu M, Zeng X, Song Q, Liu L, Li J. Examining regeneration technologies for etching solutions: A critical analysis of the characteristics and potentials. *J Clean Prod.* 2016; 113: 973–980.